Electronic Supplementary Material (ESI) for Journal of Materials Chemistry C.


# A New Photo Switchable Azobenzene Macrocycle Without Thermal Relaxation at Ambient Temperature

Nadi Eleya,[+a,b,c] Souvik Ghosh,[+a,b] Enno Lork,[d] and Anne Staubitz*[,a,b]

[a] University of Bremen, Institute for Organic and Analytical Chemistry, Leobener Str. 7, 28359 Bremen, Germany

[b] University of Bremen, MAPEX Center for Materials and Processes, Bibliothekstr. 1, 28359 Bremen, Germany

[c] Department of Chemistry, Faculty of Science, University of Zakho, KIR, Iraq

[d] University of Bremen, Institute of Inorganic Chemistry and Crystallography, Leobener Str. 7, 28359 Bremen, Germany

[+] These authors contributed equally to this work.

* staubitz@uni-bremen.de

# Supporting Information

## Table of Contents

# 1. General Information

## 1.1 Analyses

$^{1}$H NMR, $^{13}$C{$^{1}$H} NMR spectra were recorded at 298 K. $^{1}$H NMR spectra were recorded on a Bruker DRX 600 (600 MHz) spectrometer. $^{1}$H NMR spectra were recorded at 600 MHz, $^{13}$C{$^{1}$H} NMR spectra at 151 MHz. All $^{1}$H NMR and $^{13}$C{$^{1}$H} NMR spectra were referenced to the residual proton signals of the solvent ($^{1}$H), the solvent itself ($^{13}$C) or against tetramethylsilane (TMS). All chemical shifts $\delta$ are given in parts per million (ppm) and all coupling constants $J$ in Hz.

Electron Impact (EI) ionization mass spectra were obtained on the double focusing mass spectrometer MAT 95+ or MAT 8200 from Finnigan Mat. Samples were measured by direct inlet or indirect inlet method with a source temperature of 200 °C. The ionization energy of the electron impact ionization was 70 eV. All signals were reported with the quotient from mass to charge $m/z$. High resolution (HR) mass spectra were recorded on the double focusing mass spectrometer MAT 95+ from Finnigan Mat. Precision weights were determined with the peak matching method. The reference substance was perfluorokerosene (PFK). The resolution (R) of the peak-matching performance was 10 000. The calculated isotopic distribution for each ion was in agreement with experimental values.

IR spectra were recorded on a Nicolet Thermo iS10 Scientific IR spectrometer with a diamond-ATR-unit. The resolution was 4 $cm^{-1}$. Relative intensities of the IR bands were described by s = strong, m = medium or w = weak.

UV/Vis spectra were recorded with a resolution of 0.1 nm on a UV-2700 spectrometer from Shimadzu with a double monochromator. The solvent was chloroform.

Melting points were determined on a Büchi Melting Point M-560 device. The heating rate was set to 5 K / min.

Thermal analyses were performed on a standalone Mettler Toledo DSC 3+ STAR or a Mettler Toledo TGA/DSC 3+ system for which 100 µL aluminum crucibles were used at heating rate of 10 K / min under a nitrogen flow of 20 mL / min.

Thin layer chromatography (TLC) was carried out on aluminum plates coated with silica gel 60 F254 with a layer thickness of 0.2 mm from Fluka or Macherey-Nagel. All bands were detected by using a fluorescent lamp (254 nm and 366 nm). Column chromatography was carried out by using the column machine PuriFlash 4250 from Interchim. Silica gel columns of the type PF (PuriFlash) -15 (µm grain size) SiHP (Silica gel High Performance) -F0012 (gram), PF-15SiHP-F0025, PF-50SiHP-JP-F0080, and PF-50SiHP-JPF0120 were used. The sample was applied using a dry load method. The column material of the dry load was Celite 503 from Macherey-Nagel.

X-Ray measurements were carried out at 100 K on a Bruker Venture D8 diffractometer (Bruker, Karlsruhe, Germany) with Mo-Kα (0.7107 Å) radiation. All structures were solved by intrinsic phasing and refined based on F2 by use of the SHELX program package, as implemented in OLex 1.2. All non-hydrogen atoms were refined using anisotropic displacement parameters. Hydrogen atoms attached to carbon atoms were included in geometrically calculated positions using a riding model. All crystals were obtained by slow evaporation of a heptane/ethanol mixture at 25 °C.

1.2 Reagents

| **Reagent** | **Supplier** | **Purity** |
|---|---|---|
| 2-Aminophenol | TCI | >98% |
| Di-*tert*-butyldicarbonate | Alfa Aesar | 97% |
| 1,2-Bis(bromomethyl)benzene | Chempur | 97% |
| Manganese dioxide | TH. GEYER | 99% |
| Magnesium sulfate | Grüssing | 99% |
| Potassium carbonate | Sigma Aldrich | 99% |
| Sodium carbonate | Sigma Aldrich | 99% |
| Tetrabutylammonium bromide | Sigma Aldrich | >98% |
| Trifluoroacetic acid | Sigma Aldrich | 99% |
| Sodium chloride | Grüssing | 99.5% |

## 1.2 Solvents

| **Solvent** | **Supplier** | **Comments** |
|---|---|---|
| Dichloromethane | VWR | for HPLC; dry, from the SPS and degassed |
| Acetonitrile | VWR | for HPLC; dry, from the SPS and degassed |
| Ethyl acetate | Fischer Chemicals | 99.97% |
| Hexane | VWR | distilled |
| Methanol | Sigma Aldrich | 99% |
| Pentane | VWR | distilled |
| Toluene | VWR | for HPLC; dry, from the SPS and degassed |
| Triethylamine | abcr | 99% |

# 2. Syntheses

## tert-Butyl (2-hydroxyphenyl)carbamate (**2**)[1]

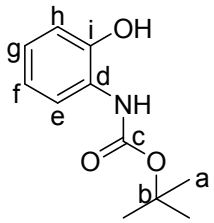


2-Aminophenol (5.00 g, 45.8 mmol) and triethylamine (11.50 mL, 68.73 mmol) were dissolved in methanol (75 mL). Di-*tert*-butyldicarbonate (10.99 g, 50.40 mmol) was added in one portion to the reaction mixture, which was stirred for 4 h at 20 °C. Subsequently, the solvent was removed in vacuo, and the residue was purified by column chromatography on silica gel (cyclohexane : ethyl acetate = 4 : 1 , $R_f$ = 1.9) to afford the desired product (**2**) as a yellow solid (6.80 g, 71%).

**m.p.** 146-147 °C.

**IR (ATR)** $\tilde{\nu}$ = 3425 (w), 3284 (br), 2984 (w), 2967 (w), 1687 (s), 1612 (m), 1595 (m), 1519 (s), 1454 (s), 1393 (m), 1369 (m), 1343 (m), 1324 (s), 1283 (m), 1270 (m), 1248 (m), 1223 (s), 1189 (s), 1146 (s), 1109 (s), 1053 (s), 1038 (m), 1027 (s), 927 (w), 896 (w), 841 (w), 812 (w), 775 (m), 761 (w), 748 (s), 734 (s) $cm^{-1}$.

**$^1$H NMR (601 MHz, $CDCl_3$)** δ 8.15 (s, 1H, NH), 7.13 – 7.02 (m, 2H, $H_e$, $H_g$), 6.99 (d, $J$ = 8.2, 1.6 Hz, 1H, $H_h$), 6.88 (ddd, $J$ = 7.6, 1.4 Hz, 1H, $H_f$), 6.67 (s,1H, OH), 1.55 (s, 9H, $H_a$) ppm.

**$^{13}$C{$^1$H} NMR (151 MHz, $CDCl_3$)** δ 155.08 ($C_i$), 147.61 ($C_c$), 125.74 ($C_g$), 125.55 ($C_d$), 121.49 ($C_e$), 120.76 ($C_f$), 119.03 ($C_h$), 82.15 ($C_b$), 28.13 ($C_a$) ppm.

**EI** *m/z* (% relative intensity): 209 (4) $[M]^+$, 57 (100).

**HRMS (EI)** *m/z* for $C_{11}H_{15}NO_3$ $[M]^+$: calcd. 209.10483, found: 209.10464.

## *di*-*tert*-Butyl(((1,2-phenylenebis(methylene))bis(oxy))bis(2,1-phenylene))dicarbamate (**4**)

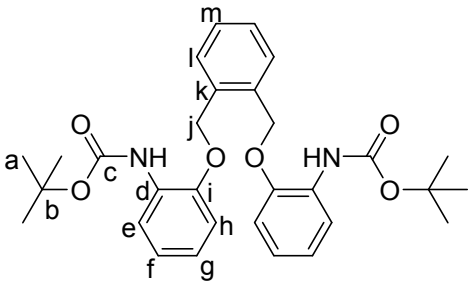


*tert*-Butyl (2-hydroxyphenyl)carbamate (**2**) (400 mg, 1.91 mmol), potassium carbonate (634 mg, 4.58 mmol), tetrabutylammonium bromide (30.8 mg, 5 mol%) and 1,2-bis(bromomethyl)benzene (**3**) (252 mg, 955 µmol) were suspended in acetonitrile (10 mL). The reaction mixture was stirred for 8 h at 80 °C and for 16 h at 20 °C. Subsequently, the solid was removed by filtration and the product was extracted with ethyl acetate (3 x 30 mL). The organic phase was washed consecutively with water (2 × 10 mL) and brine (2 × 10 mL). The extracts were dried over anhydrous $MgSO_4$, filtered and the solvent was removed in vacuo. Subsequently, the crude product was purified by column chromatography on

silica gel (cyclohexane : ethyl acetate = 4 : 1,$R_f$ = 1.7) to obtain the desired product (**4**) as yellow oil (448 mg, 90%).

**IR (ATR)** $\tilde{\nu}$ = 3425 (w), 3291 (br), 2983 (w), 2967 (w), 2930 (w), 1691 (m), 1611 (m), 1597 (w), 1515 (s), 1454 (s), 1393 (w), 1369 (m), 1344 (w), 1324 (m), 1281 (w), 1270 (w), 1247 (m), 1221 (s), 1190 (w), 1141 (s), 1108 (s), 1051 (s), 1026 (s), 926 (m), 896 (m), 812 (m), 774 (s), 747 (s), 734 (s) $cm^{-1}$.

**$^1$H NMR (601 MHz, $CDCl_3$)** δ 8.11 (d, *J* = 7.6 Hz, 1H, $H_e$), 7.51-7.47 (m*, 1H, $H_l$), 7.45-7.41 (m*, 1H, $H_g$), 7.15 (s, 1H, NH), 7.03 – 6.93 (m, 3H, $H_m$, $H_h$, $H_f$), 5.23 (s, 2H, $H_j$), 1.47 (s, 9H, $H_a$) ppm.

* in higher order

**$^{13}$C{$^1$H} NMR (151 MHz, $CDCl_3$)** δ 152.76 ($C_i$), 146.57 ($C_d$), 134.86 ($C_k$), 129.61 ($C_g$), 128.93 ($C_l$), 122.44 ($C_m$), 121.99 ($C_f$), 118.70 ($C_h$), 112.34 ($C_e$), 80.35 ($C_b$) 69.18 ($C_j$), 28.28 ($C_a$) ppm.

**EI** *m/z* (% relative intensity): 520 (10 ($[M]^+$), 104 (100).

**HRMS (EI)** *m/z* for $C_{30}H_{36}N_2O_6$ $[M]^+$: calcd. 520.25739, found: 520.25679.

## 2,2'-((1,2-Phenylenebis(methylene))bis(oxy))dianiline (**5**)

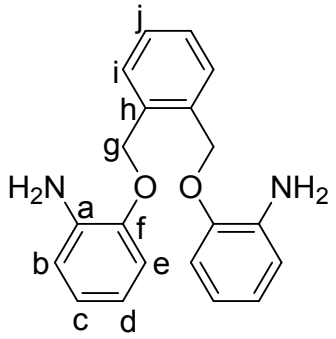


A 50 mL oven-dried flask was charged with 2,2'-((1,2-phenylenebis(methylene))bis(oxy))dianiline (**4**) (400 mg, 770 µmol) in dichloroethane (20 mL). The resulting solution was cooled to 0 °C followed by the drop-wise addition (over 5 minutes) of trifluoroacetic acid *(*TFA*)* (1.10 mL, 15.4 mmol). The reaction mixture was allowed to warm to 20 °C and was stirred at this temperature for 2 h to consume the starting material completely (monitored by TLC). After removal of the solvent under reduced pressure, the residue was dissolved in DCM (20 mL) and the mixture was neutralized with a saturated aqueous solution of $Na_2CO_3$ solution to pH = 8. The organic layer was separated and the aqueous layer was extracted with DCM (2 x 20 mL). The combined organic layers were washed with water (2 x 20 mL) and brine (3 x 20 mL). The extracts were dried over anhydrous $MgSO_4$, filtered, and concentrated under reduced pressure. Subsequently, the crude product was purified by column chromatography on silica gel (cyclohexane : ethyl acetate = 4 : 1, $R_f$ = 2.5) to obtain the desired product (**5**) as a red oil (205 mg, 83%).

**IR (ATR)** $\tilde{\nu}$ = 3450 (w), 3362 (w), 3031 (w), 2924 (w), 1770 (w), 1611 (m), 1501 (s), 1457 (m), 1380 (w), 1339 (w), 1273 (s), 1203 (s), 1140 (m), 1071 (w), 1038 (m), 1004 (s), 947 (w), 908 (w), 882 (w), 850 (w), 791 (w), 733 (s) $cm^{-1}$.

**$^1$H NMR (601 MHz, $CDCl_3$)** δ 7.55-7.51 (m*, 1H, $H_b$), 7.41-7.37 (m*, 1H, $H_i$), 6.90 (dd, *J* = 8.0, 1.3 Hz, 1H, $H_d$), 6.84 (dd, *J* = 7.6, 1.3 Hz, 1H, $H_j$), 6.78 – 6.69 (m, 2H, $H_e$, $H_c$), 5.20 (s, 2H, $H_g$), 3.79 (s, 2H, $NH_2$).

* in higher order

**$^{13}C\{^1H\}$ NMR (151 MHz, $CDCl_3$)** δ 146.28 ($C_f$), 136.63 ($C_a$), 135.42 ($C_h$), 129.22 ($C_d$), 128.50 ($C_i$), 121.73 ($C_j$), 118.39 ($C_c$), 115.27 ($C_e$), 112.31 ($C_b$), 68.35 ($C_g$) ppm.

**EI** *m/z* (% relative intensity): 320 (15 ($[M]^+$), 212 (100).

**HRMS (EI)** *m/z* for $C_{20}H_{20}N_2O_2$ $[M]^+$: calcd. 320.15234, found: 320.15193.

## (*E*)-12,17-Dihydrotribenzo[b,f,j][1,8]dioxa[4,5]diazacyclododecine (**6**)

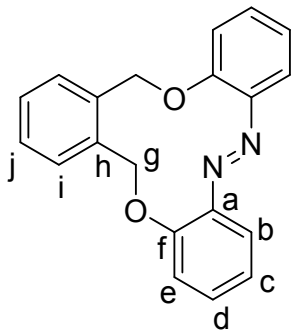


2,2'-((1,2-Phenylenebis(methylene))bis(oxy))dianiline (**5**) (200 mg, 625 µmol) was dissolved in dry toluene (6 mL). Dried $MnO_2$ (135 mg, 2.50 mmol) was added and the suspension was heated to reflux for 4 hours. The reaction mixture was allowed to cool and again dried activated $MnO_2$ (0.101 g, 1.88 mmol) was added to the reaction mixture. The suspension was heated to reflux for another 4 h. Then the reaction mixture was allowed to reach room temperature (20 °C) and was then diluted with DCM (10 mL). The reaction mixture was filtered through celite. The filtrate was evaporated to dryness under reduced pressure, and the residue was chromatographed on silica gel with (cyclohexane : ethyl acetate = 4:1, $R_f$ = 3.1) as eluent, to obtain final compound (**6**) (177 mg**,** 89**%**) enriched in the *E* form (*E*: 98%, *Z*: 2%) as an orange solid.

**m. p.** 133-134 °C.

**IR (ATR):** $\tilde{\nu}$ = 2898 (w), 1908 (w), 1591 (w), 1568 (w), 1489 (w). 1475 (m), 1465 (s), 1441 (w), 1431 (w), 1364 (w), 1331 (m), 1294 (w), 1262 (s), 1246 (w), 1213 (m), 1200 (m), 1149 (m), 1112 (w), 1103 (m), 1043 (m), 1015 (w), 978 (m), 945 (m), 863 (w), 844 (w), 789 (m), 778 (w), 753 (s), 736 (s), 721 (s). 711 (m) $cm^{-1}$.

**$^1H$ NMR (601 MHz, $CDCl_3$)** δ 7.81 (dd, *J* = 7.9, 1.7 Hz, 1H, $H_b$), 7.51-7.47 (m*, 1H, $H_i$), 7.39 (dd, *J* = 7.8, 1.2 Hz, 1H, $H_j$), 7.37 – 7.33 (m, 1H, $H_d$), 7.31 (dd, *J* = 8.1, 1.1 Hz, 1H, $H_e$), 7.25 – 7.23 (m, 1H, $H_c$), 5.38 (s, 2H, $H_g$).

* in higher order

**$^{13}C\{^1H\}$ NMR (151 MHz, $CDCl_3$)** δ 152.92 ($C_f$), 146.25 ($C_a$), 136.81 ($C_h$), 131.76 ($C_d$), 131.47 ($C_i$), 128.95 ($C_j$), 124.43 ($C_c$), 124.14 ($C_e$), 123.42 ($C_b$), 76.81 ($C_g$) ppm.

**EI** *m/z* (% relative intensity): 316 (3 ($[M]^+$), 209 (100).

**HRMS (APCI)** *m/z*: $C_{20}H_{17}N_2O_2$ $[M+H]^+$: calcd. 317.12845 found: 317.12824.

# 3. NMR Spectra

## $^{1}H$ NMR and $^{13}C\{^{1}H\}$ NMR spectra of compound **2**

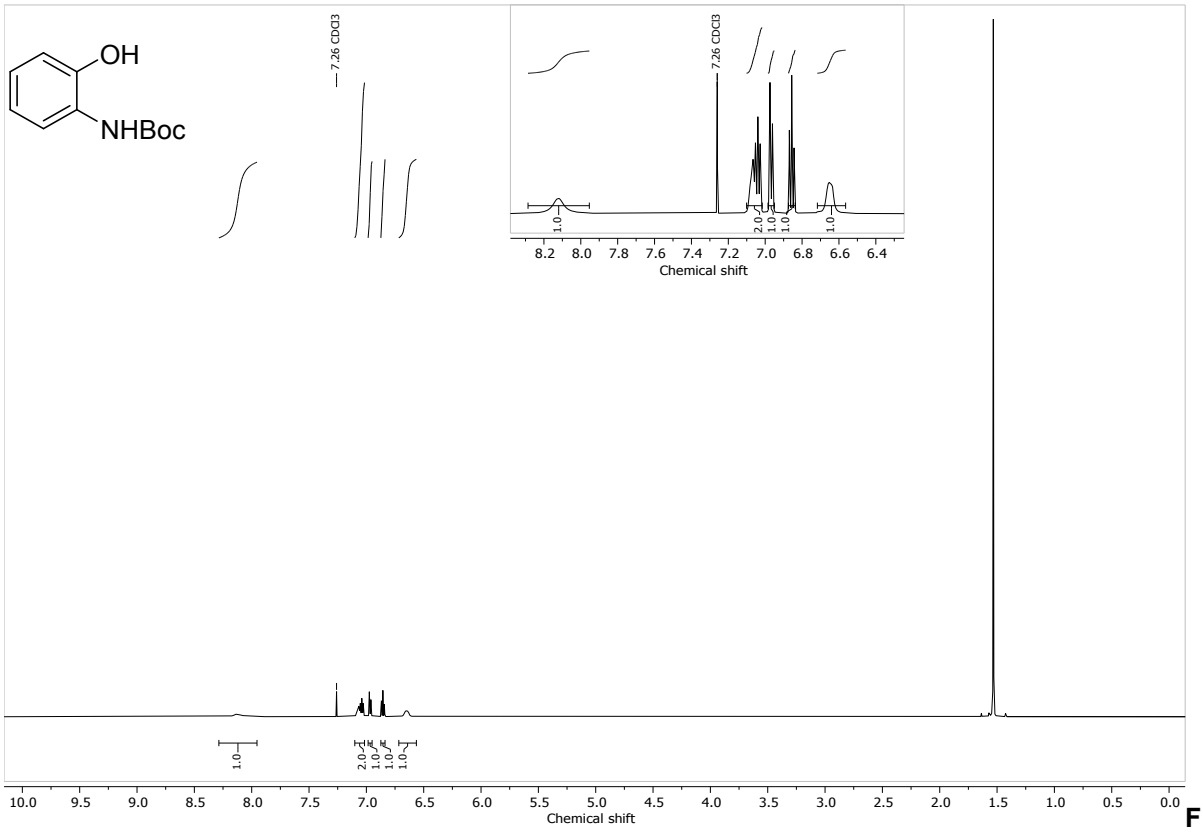


**igure S1.** $^{1}H$ NMR (600 MHz) spectrum of **2** in $CDCl_3$.

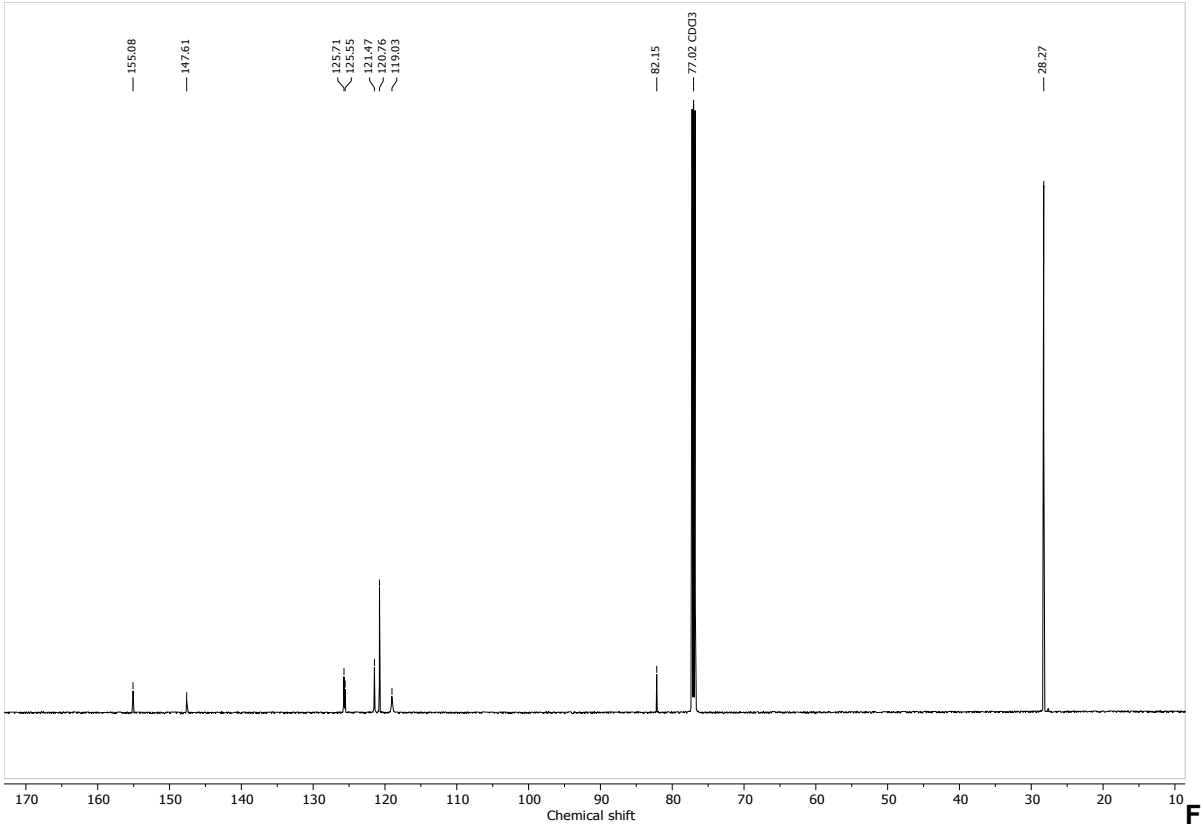


**igure S2.** $^{13}C\{^{1}H\}$ NMR (156 MHz) spectrum of **2** in $CDCl_3$.

$^{1}$H NMR and $^{13}$C{$^{1}$H} NMR spectra of compound **4**

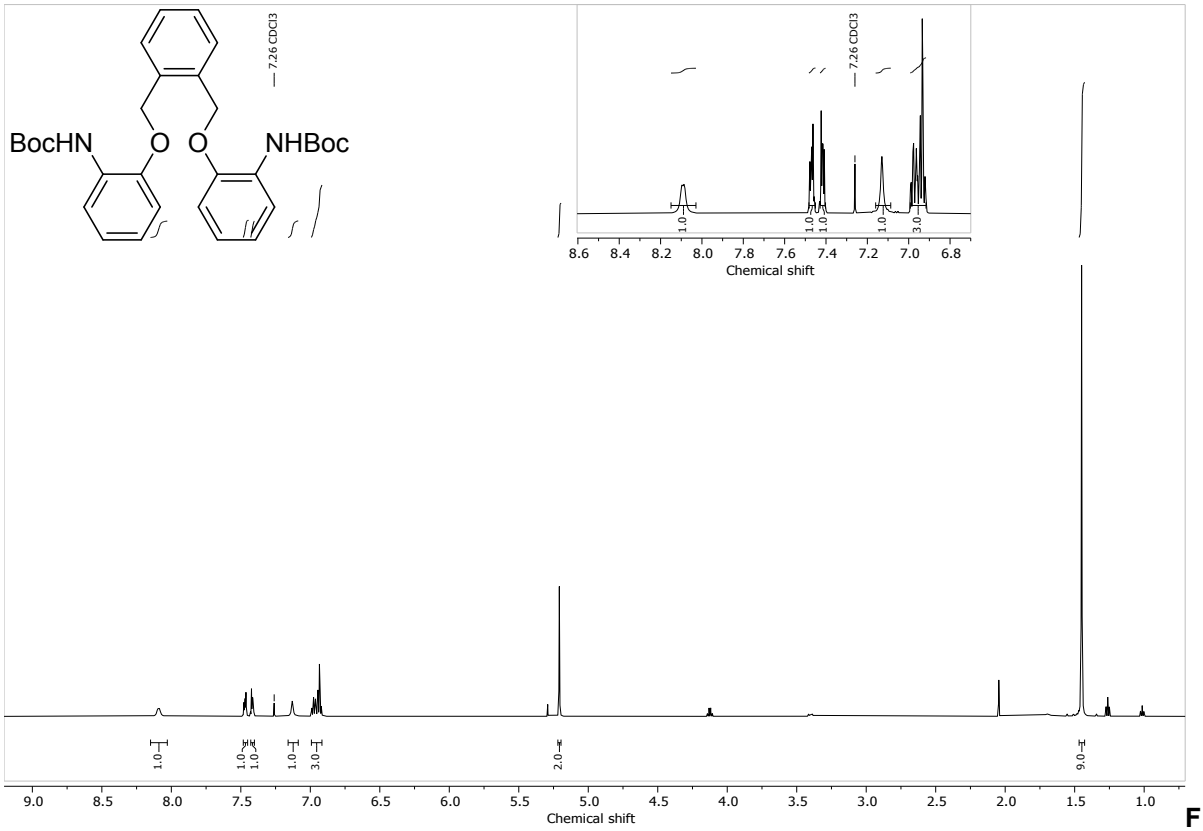


**F**

**igure S3.** $^{1}$H NMR (600 MHz) spectrum of **4** in $CDCl_3$.

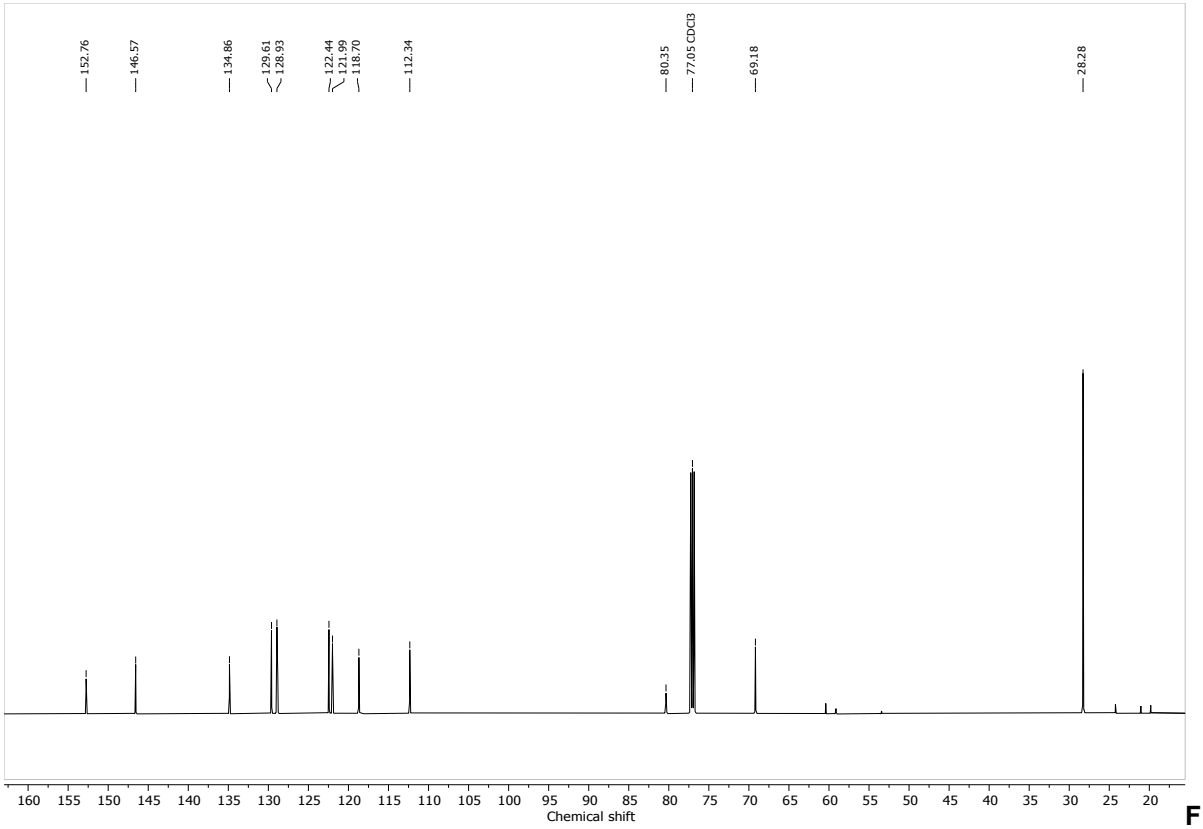


**F**

**igure S4.** $^{13}$C{$^{1}$H} NMR (151 MHz) spectrum of **4** in $CDCl_3$.

## $^{1}H$ NMR and $^{13}C$ $\{^{1}H\}$ NMR spectra of compound **5**

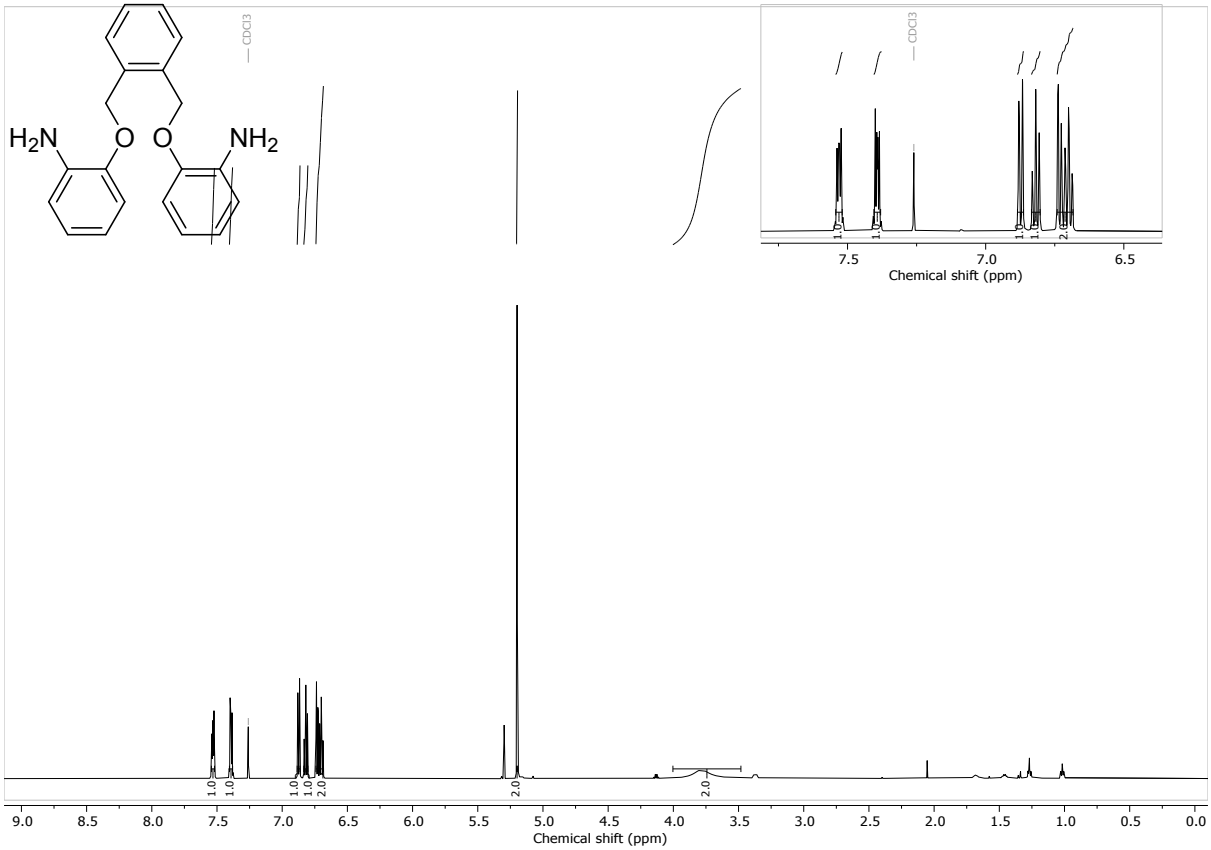


**Figure S5.** $^{1}H$ NMR (600 MHz) spectrum of **5** in $CDCl_3$.

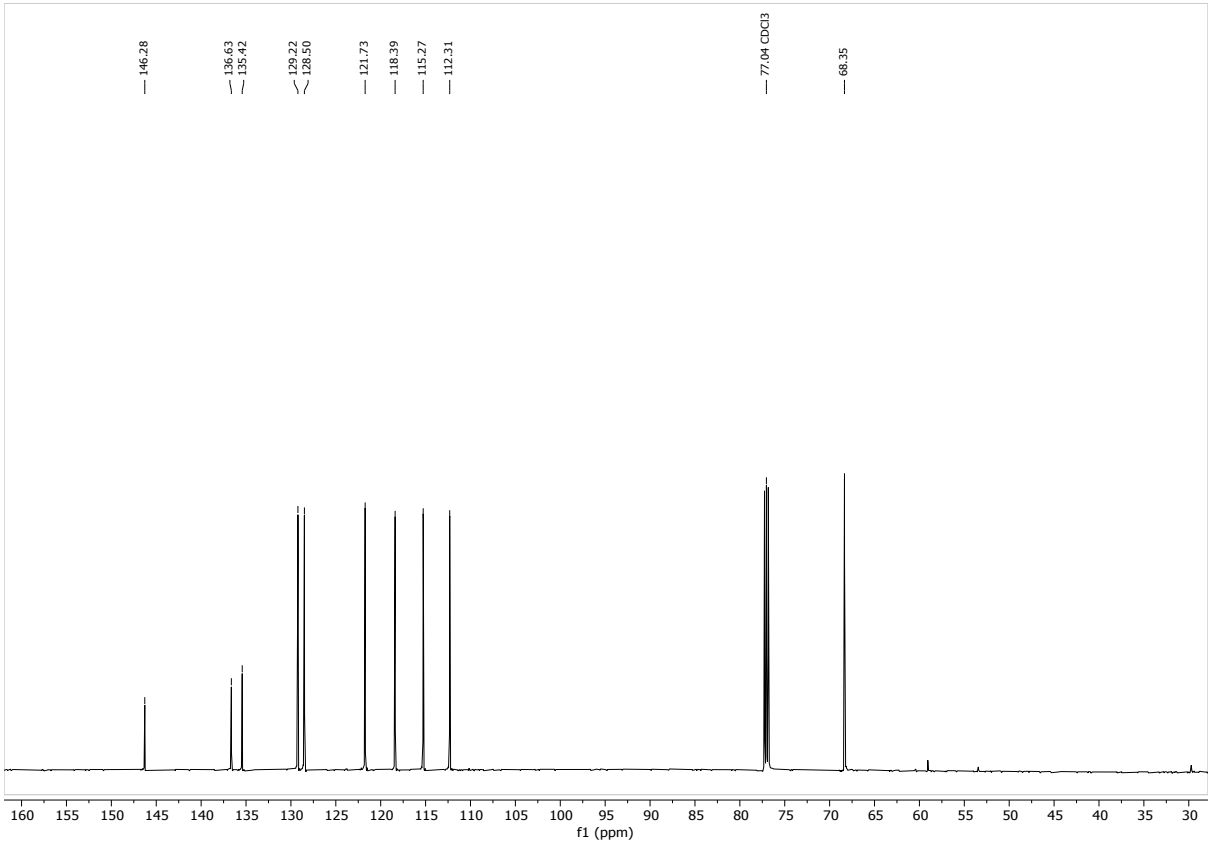


**Figure S6.** $^{13}C\{^{1}H\}$ NMR (151 MHz) spectrum of **5** in $CDCl_3$.

$^{1}$H NMR and $^{13}$C {$^{1}$H} NMR spectra of compound **6(*E*)**

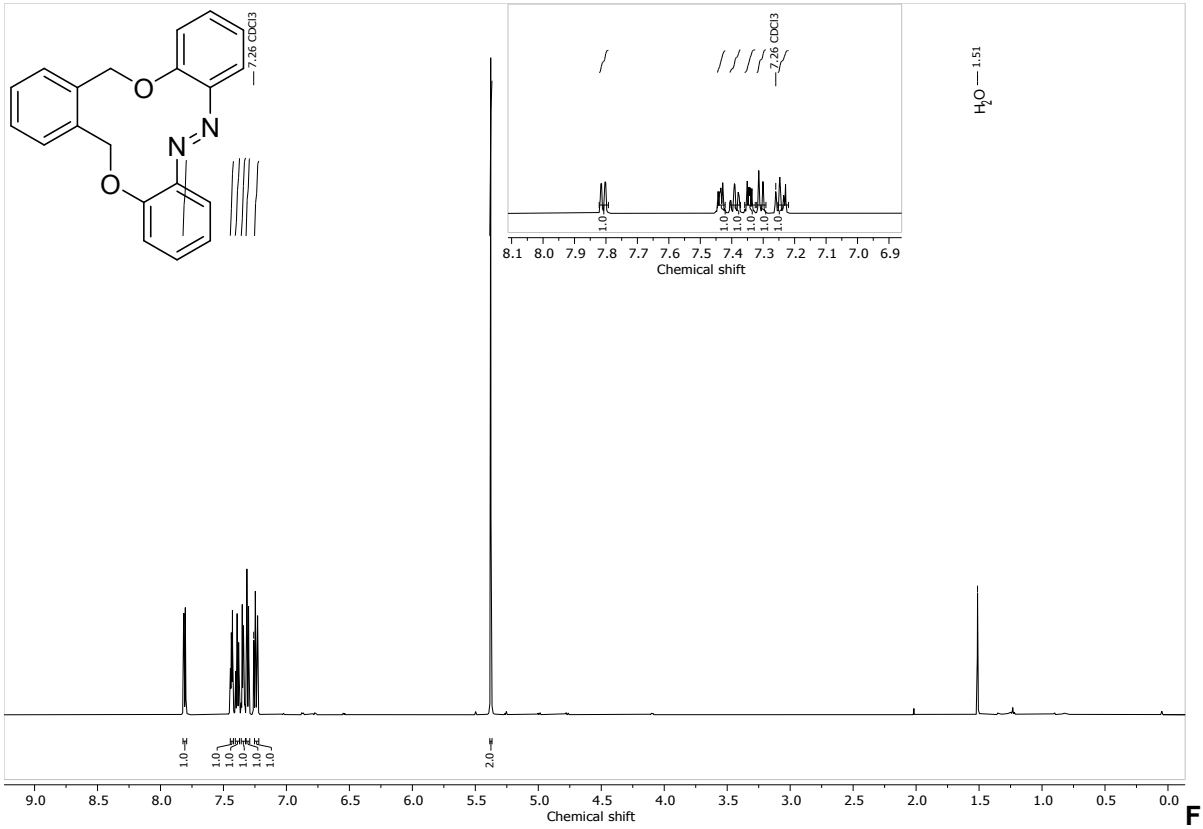


**igure S7.** $^{1}$H NMR (600 MHz) spectrum of **6(*E*)** in $CDCl_3$

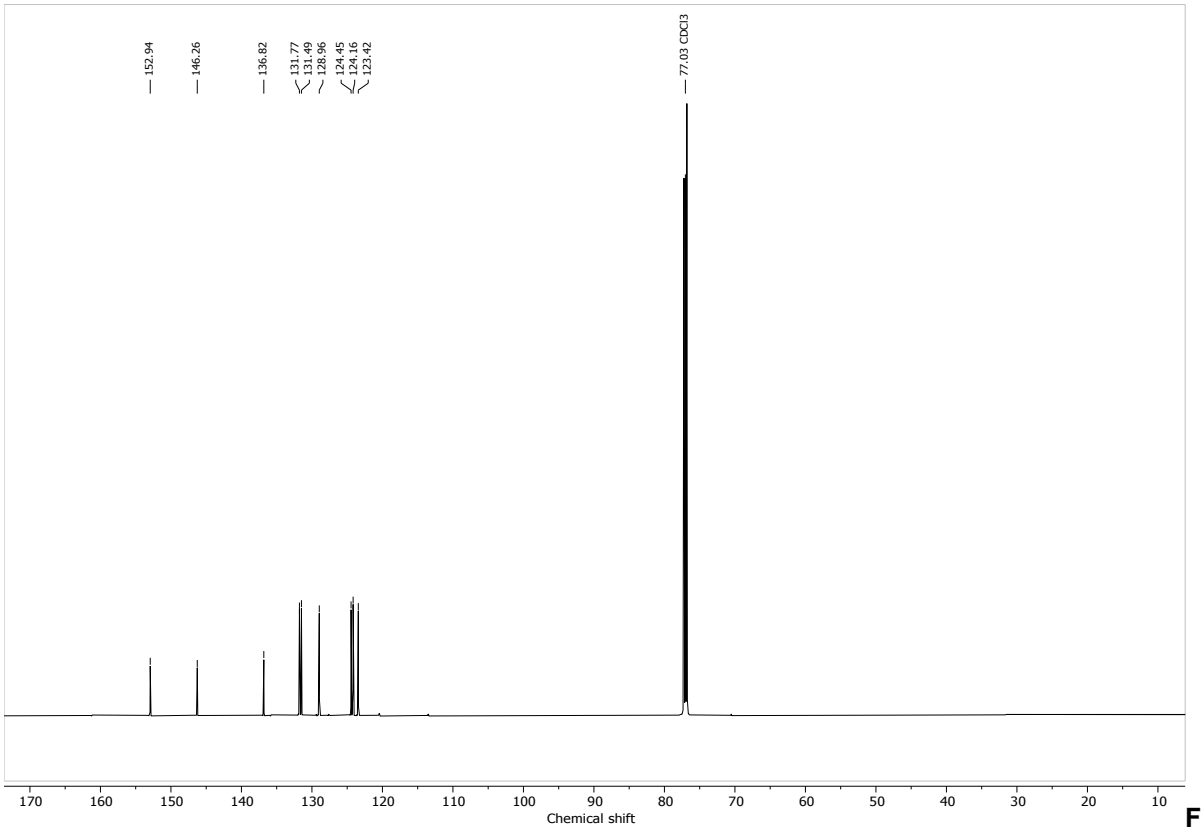


**igure S8.** $^{13}$C{$^{1}$H} NMR (151 MHz) spectrum of **6(*E*)** in $CDCl_3$.

# 4. Summary of the Crystal Data for Compounds **6(*E*)** and **6(*Z*)**

**Table S1.** Crystal data and structure refinement for **6(*E*)**.

| | |
|---|---|
| Empirical formula | $C_{20}H_{16}N_2O_2$ |
| Formula weight | 316.35 |
| Temperature/K | 100.0 |
| Crystal system | orthorhombic |
| | |
| Space group | $P2_12_12_1$ |
| a/Å | 5.2398(2) |
| b/Å | 9.5789(3) |
| c/Å | 30.1769(10) |
| α/° | 90 |
| β/° | 90 |
| γ/° | 90 |
| Volume/Å$^3$ | 1514.62(9) |
| Z | 4 |
| $\rho_{calc}$g/cm$^3$ | 1.387 |
| μ/mm$^{-1}$ | 0.091 |
| F(000) | 664.0 |
| Crystal size/mm$^3$ | 0.24 × 0.2 × 0.18 |
| Radiation | MoKα (λ = 0.71073) |
| 2Θ range for data collection/° | 6.874 to 59.352 |
| Index ranges | -7 ≤ h ≤ 6, -12 ≤ k ≤ 13, -40 ≤ l ≤ 42 |
| Reflections collected | 29627 |
| Independent reflections | 4290 [$R_{int}$ = 0.0300, $R_{sigma}$ = 0.0210] |
| Data/restraints/parameters | 4290/0/217 |
| Goodness-of-fit on $F^2$ | 1.069 |
| Final R indexes [I>=2σ (I)] | $R_1$ = 0.0375, $wR_2$ = 0.0870 |
| Final R indexes [all data] | $R_1$ = 0.0399, $wR_2$ = 0.0881 |
| Largest diff. peak/hole / e Å$^{-3}$ | 0.31/-0.24 |
| Flack parameter | 0.3(2) |

**Table S2.** Crystal data and structure refinement for **6(*Z*)**.

| | |
|---|---|
| Empirical formula | $C_{20}H_{16}N_2O_2$ |
| Formula weight | 316.35 |
| Temperature/K | 100.0 |
| Crystal system | triclinic |
| Space group | P-1 |
| a/Å | 11.2809(10) |
| b/Å | 11.8263(8) |
| c/Å | 12.9517(10) |
| α/° | 74.483(3) |
| β/° | 71.717(3) |
| γ/° | 75.701(4) |
| Volume/Å$^3$ | 1555.6(2) |
| Z | 4 |
| $\rho_{calc}$g/cm$^3$ | 1.351 |
| μ/mm$^{-1}$ | 0.089 |
| F(000) | 664.0 |
| Crystal size/mm$^3$ | 0.2 × 0.2 × 0.2 |
| Radiation | MoKα (λ = 0.71073) |
| 2Θ range for data collection/° | 4.81 to 56.72 |
| Index ranges | -15 ≤ h ≤ 15, -15 ≤ k ≤ 15, -17 ≤ l ≤ 17 |
| Reflections collected | 31945 |
| Independent reflections | 7723 [$R_{int}$ = 0.0365, $R_{sigma}$ = 0.0317] |
| Data/restraints/parameters | 7723/0/434 |
| Goodness-of-fit on F$^2$ | 1.032 |
| Final R indexes [I>=2σ (I)] | $R_1$ = 0.0434, $wR_2$ = 0.0954 |
| Final R indexes [all data] | $R_1$ = 0.0594, $wR_2$ = 0.1028 |
| Largest diff. peak/hole / e Å$^{-3}$ | 0.33/-0.23 |

## 5. Thermogravimetric Analysis of **6(*E*)**

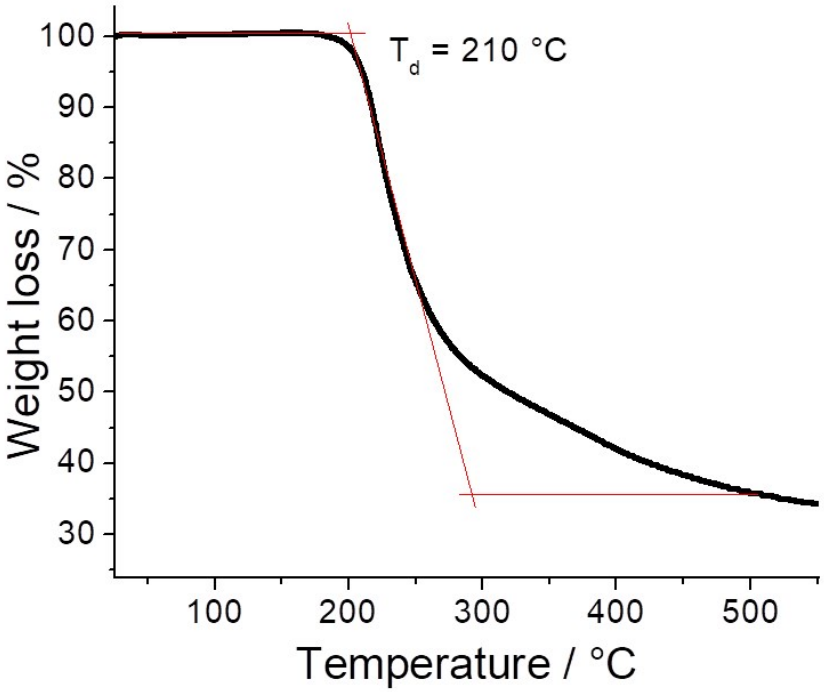


**Figure S9.** Thermogravimetric analysis (TGA) for compound **6(*E*)** at heating rate of 10 K / min under a nitrogen flow of 20 mL / min.

## 6. UV-vis Study of **6(*E*)** and **6(*Z*)**

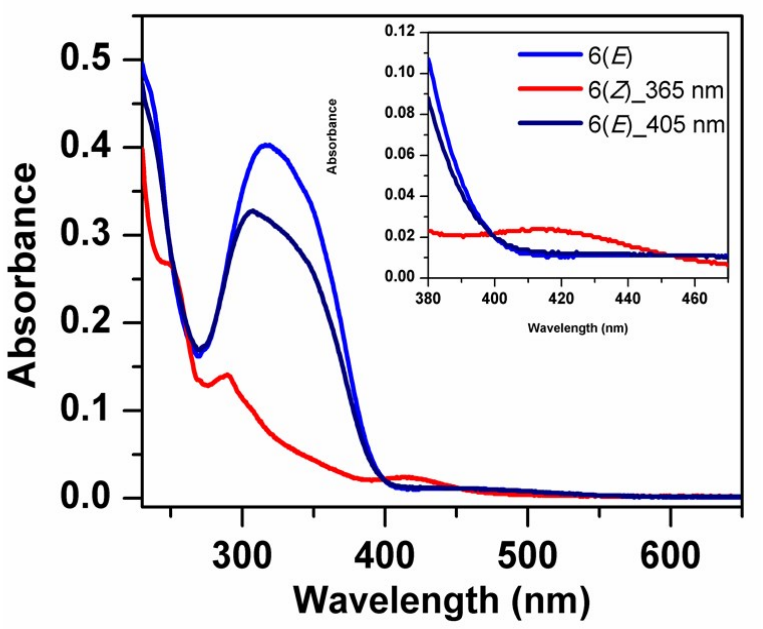


**Figure S10.** The UV/vis spectrum of **6(*E*)** (0.025 mg / mL in acetonitrile) as synthesized (light blue line); **6(*Z*)** after irradiation of that sample using a 365 nm LED light (red line); after irradiation of **6(*Z*)** using a 405 nm LED light (dark blue line). Enlargement of the visual region of the spectrum (inset top-right).

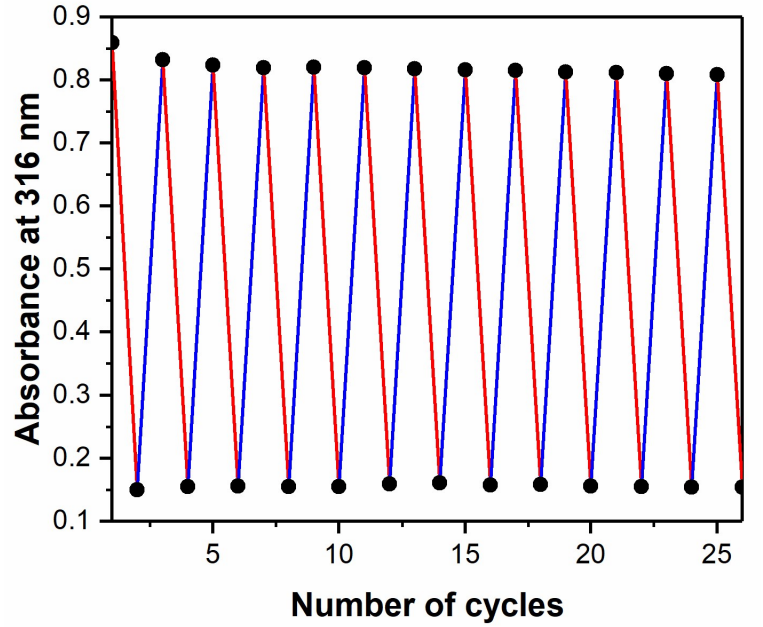


**Figure S11.** Absorptions at 316 nm with alternating irradiations at 365 and 405 nm demonstrating reversible photoisomerization cycles of compound **6** (0.035 mg / mL in acetonitrile)

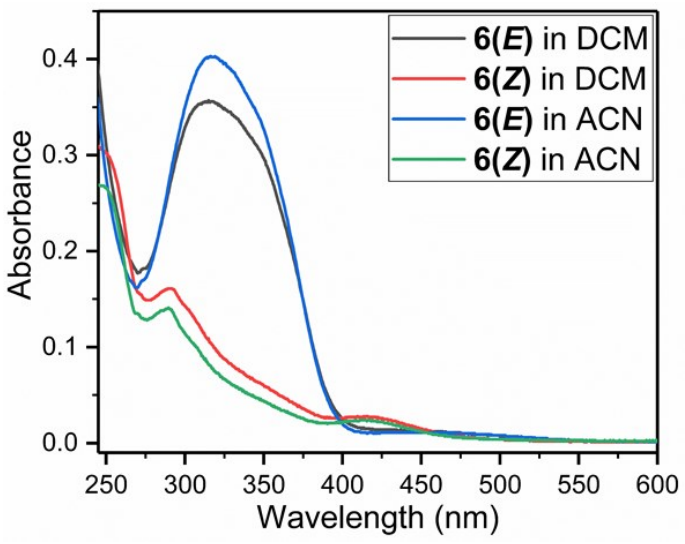


**Figure S12.** The UV/vis spectrum of **6(*E*)** (0.0125 mg / mL in dichloromethane and 0.025 mg / mL in acetonitrile): in dichloromethane (black line), in acetonitrile (blue line); **6(*Z*)** after irradiation of that sample using a 365 nm LED light: in in dichloromethane (red line), in acetonitrile (green line).

## 7. UV-vis Study of **6(*Z*)** after 120 days

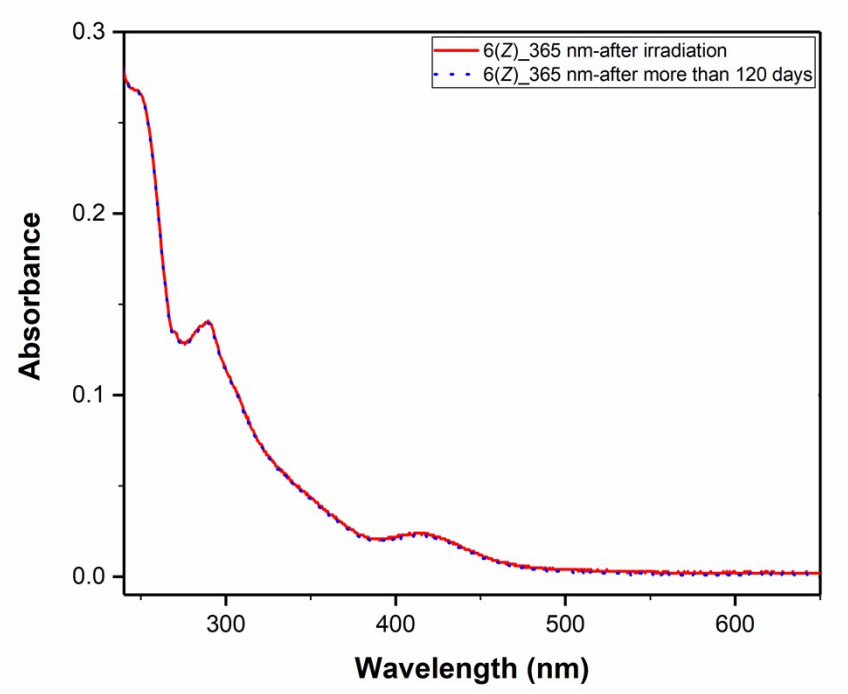


**Figure S13.** UV-vis spectra of **6(*Z*)** just after irradiation (red line) and after more than 120 days (dotted blue line).

## 8. $^1$H NMR Spectra of Compounds **6(*Z*)** and **6(*E*)**

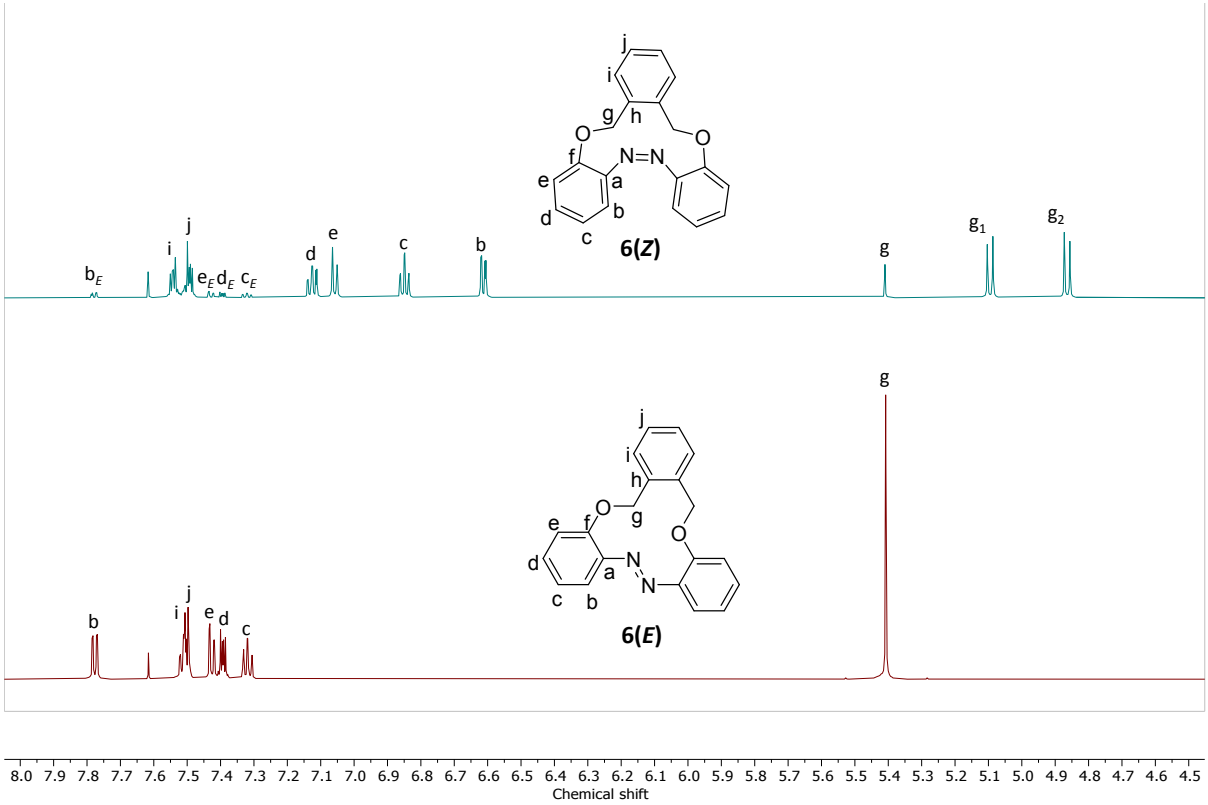


**Figure S14.** $^1$H NMR spectrum of compound **6** (2.5 mg / mL in $CD_3CN$) before and after irradiation with light at λ = 365 nm.

# 9. Kinetic Study of the Thermal Relaxation of ***6(Z)*** at Elevated Temperatures

The thermal relaxation of compound **6(*Z*)** was measured by NMR spectroscopy and by UV-vis spectroscopy at elevated temperatures.

**Measurement by NMR Spectroscopy:** Compound **6(*E*)** was dissolved in $CD_3CN$ (2.5 mg / mL) and was irradiated with LED light at a wavelength of 365 nm for 15 minutes. The samples in NMR tubes were heated at 70 °C, or 90 °C in a water bath which was shielded from light. The reactions were performed in J. Young's NMR tubes, which were hermetically sealed and can withstand a pressure of up to 13.8 bar. Therefore, it was possible to heat above the boiling point that $CD_3CN$ has at normal pressure. For spectral analysis, the NMR-tubes were removed from the water bath and placed in an NMR spectrometer at 25 °C every 60 min. The whole measurement process took 5 min each time and NMR tubes were placed in again in water bath for the ex-situ heating process (thus the measured half-lives will be slightly too high). The $^1H$ NMR spectra of **6(*Z*)** and **6(*E*)** were distinguished by a change in chemical shifts of aromatic protons. For example, the integrated peak of $H_a$ of **6(*E*)** was increased over time at 70 °C and 90 °C. (see Figure S15). The *E* to *Z* ratio was calculated by the integration of the chemically shifted proton signals in the $^1H$ NMR spectra. Thermal relaxation of **6(*Z*)** to **6(*E*)** was accomplished at 90 °C within four hours with the rate constant (k) 0.393 $h^{-1}$ assuming first order kinetics. At 70 °C, the rate constant (k) was found to be 0.019 $h^{-1}$. From the kinetics study, half-lives for transition from **6(*Z*)** to **6(*E*)** were 36.4 h and 1.76 h at 70 °C and 90 °C respectively (see Figure S15 and Figure S16).

**Measurement by UV-vis spectroscopy:** Solutions of compound **6(*E*)** with concentrations of 0.035 mg / mL and 0.030 mg / mL in acetonitrile were prepared to perform the thermal relaxation study at 70 °C and 90 °C respectively. The samples were irradiated with light at 365 nm wavelength for 90 s before placing them in water baths at 70 °C and 90 °C, shielded from light. For spectral analysis, the samples were removed from the water bath and placed in UV-vis spectrometer at 25 °C in every 60 min. The whole measurement process took 1 min each time and cuvettes were placed in again in the water bath for the ex-situ heating process. The kinetic graphs were plotted by following the intensity of absorbance of light at 316 nm wavelength during thermal relaxation of **6(*Z*)** to **6(*E*)**. Graphs of $Ln(A_t/A_0)$ vs. time showed linear curves, i.e first order reaction kinetics of the thermal relaxation. Rate constants (k) for the formation of **6(*E*)** from **6(*Z*)** were found to be 0.029 $h^{-1}$ and 0.293 $h^{-1}$ at 70 °C and 90 °C respectively. The half-lives for the transition of **6(*Z*)** to **6(*E*)** were 23.8 h and 2.35 h at 70 °C and 90 °C respectively (Figure S17). For a summary of the thermal relaxation processes see Table S3.

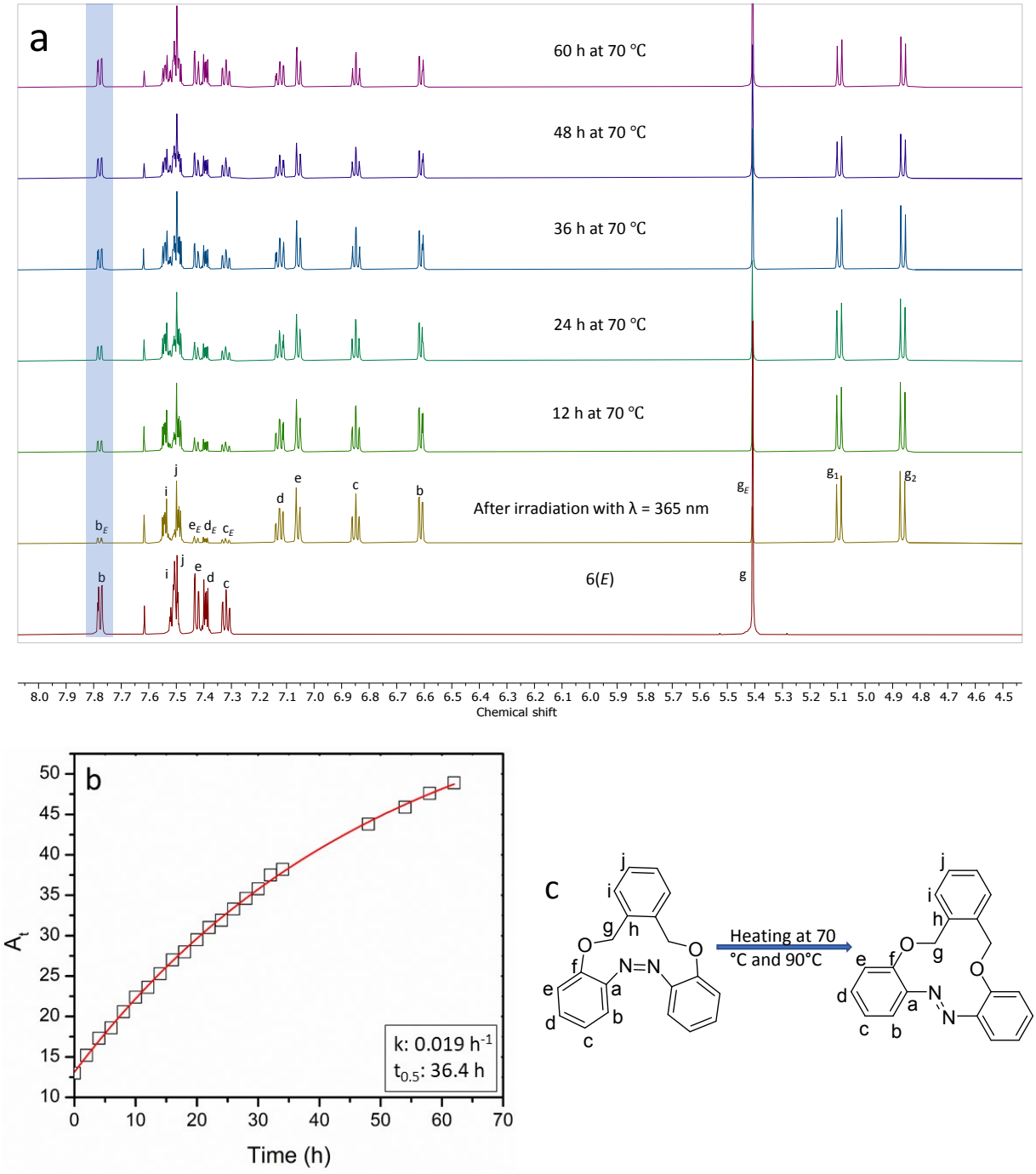


**Figure S15. a)** $^{1}$H NMR spectra of compound **6** (2.4 mg / mL in $CD_3CN$) before and after irradiation with light at 365 nm wavelength and thermal relaxation at 70 °C; **b)** $A_t$ vs. time plot of compound **6** at 70 °C; **c)** Labeling of compound **6(*E*)** and **6(*Z*)**.

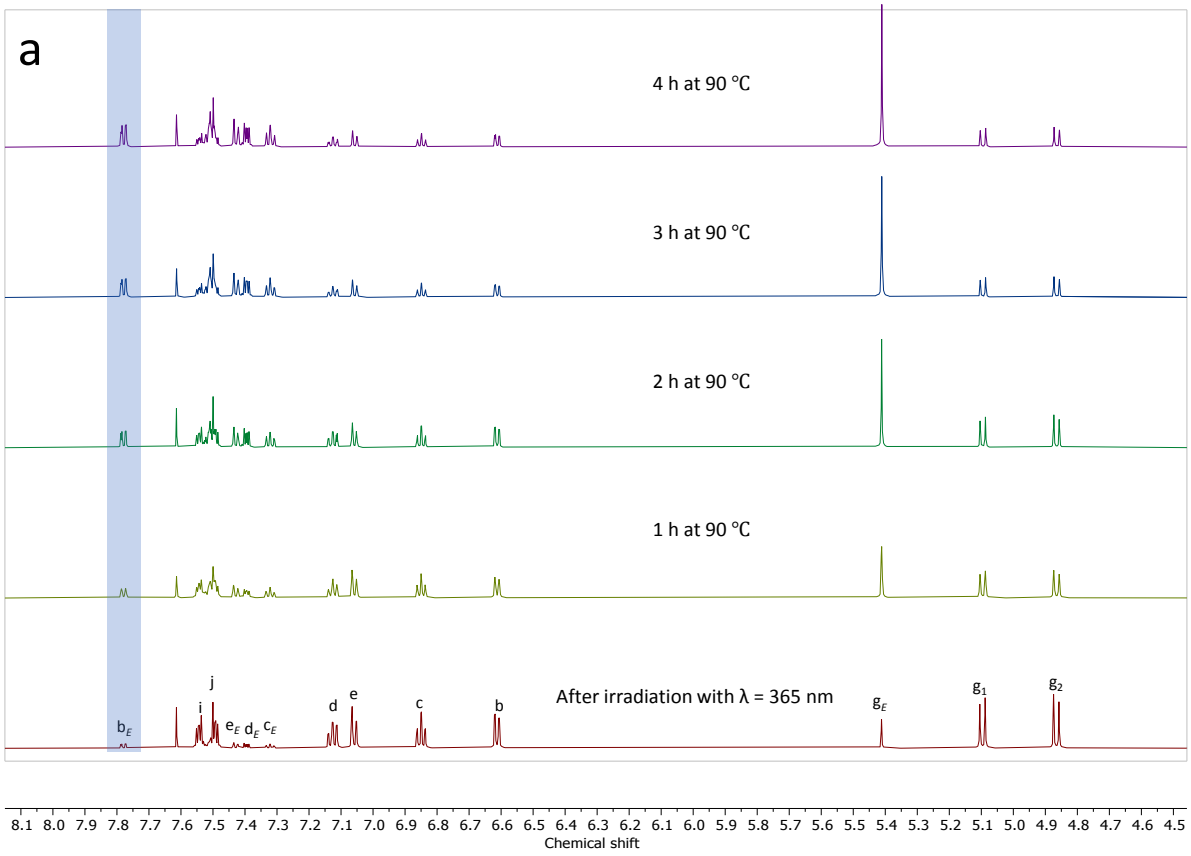


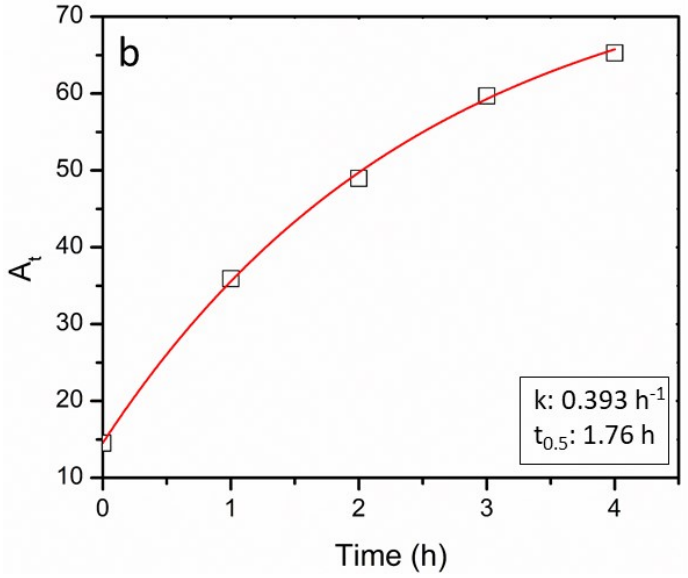


**Figure S16. a)** $^1$H NMR spectra of compound **6** (2.4 mg / mL in $CD_3CN$) before and after irradiation with light at 365 nm wavelength and thermal relaxation at 90 °C; **b)** $A_t$ vs. time plot of compound **6** at 90 °C.

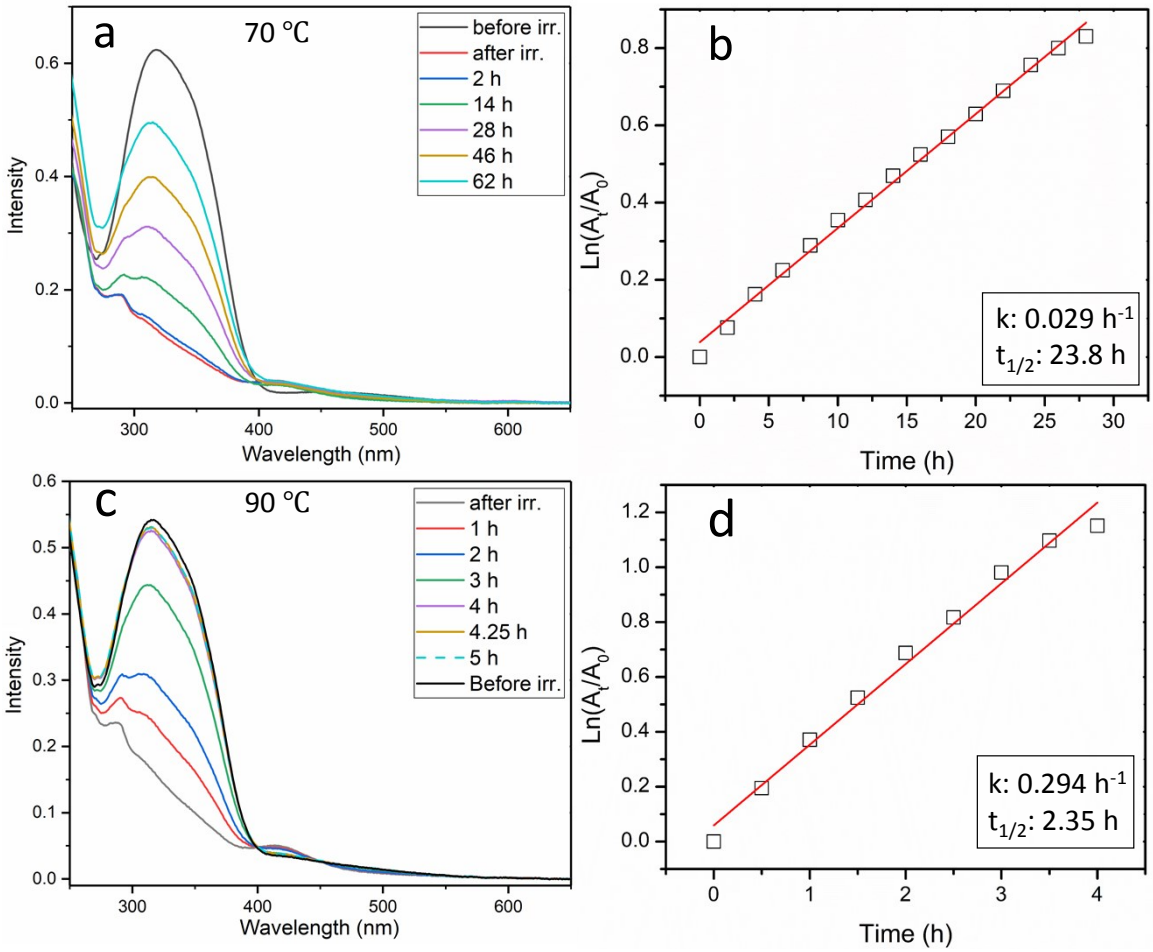


**Figure S17. a, c)** UV-vis spectra of compound **6** (0.035 mg / mL and 0.030 mg / mL in acetonitrile) before and after irradiation with light at 365 nm wavelength and thermal relaxation at 70 °C and 90 °C respectively; **b, d)** $\ln(A_t/A_0)$ vs. time plot of compound **6** at 70 °C and 90 °C.

**Table S3.** Kinetic parameters at 70 °C and 90 °C from NMR and UV-vis spectroscopy.

| **Temperature (℃)** | **Correlation coefficient ($R^2$)** | **Rate constant (k)** | **Half-life time ($t_{1/2}$)** |
|---|---|---|---|
| | | **NMR spectroscopy** | |
| **70** | 0.999 | 0.019 $h^{-1}$ | 36.4 h |
| **90** | 0.998 | 0.393 $h^{-1}$ | 1.76 h |
| | | **UV-vis spectroscopy** | |
| **70** | 0.995 | 0.029 $h^{-1}$ | 23.8 h |
| **90** | 0.988 | 0.294 $h^{-1}$ | 2.35 h |

## 10. Solid state photoisomerization of compound **6**

Solid state UV-vis study of compound **6**

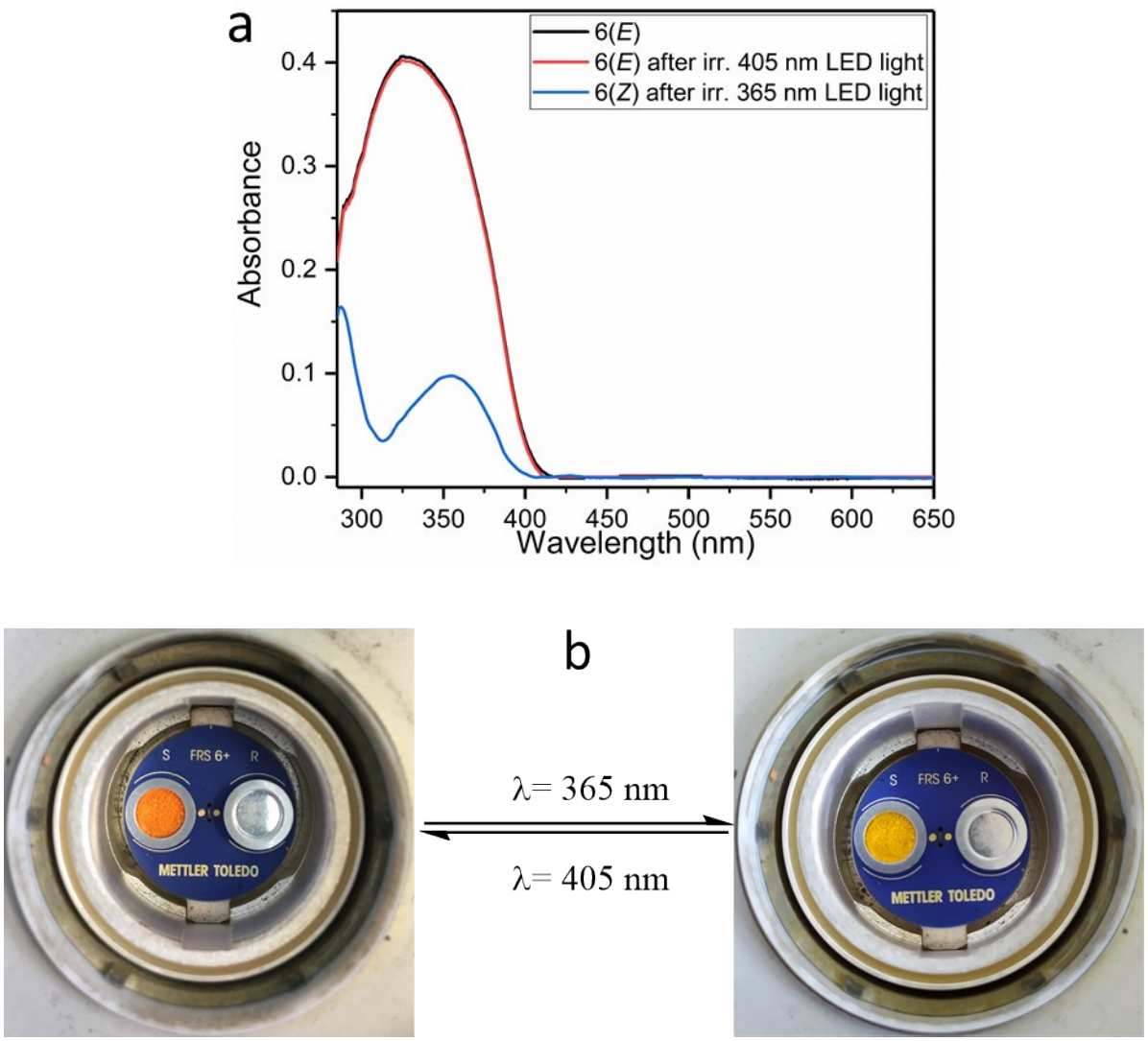


**Figure S18. a)** Solid state UV/vis spectrum of compound **6(*E*)** (black line); after irradiation of this sample using a 365 nm LED light (giving mostly **6(*Z*)**) (blue line); after irradiation of **6(*Z*)** using a 405 nm LED light (red line). **b)** Images of compound **6(*E*)** in bright orange (left side) and compound **6(*Z*)** in glossy yellow (right side). The images were taken in a DSC holder; on the left of each image, there is the sample, on the right the reference crucible.

The samples that were switched in the solid state were dissolved in $CD_3CN$ immediately after switching (Figure S19 and S20). By the integration of the peaks, we find a switching efficiency of 87.5%.

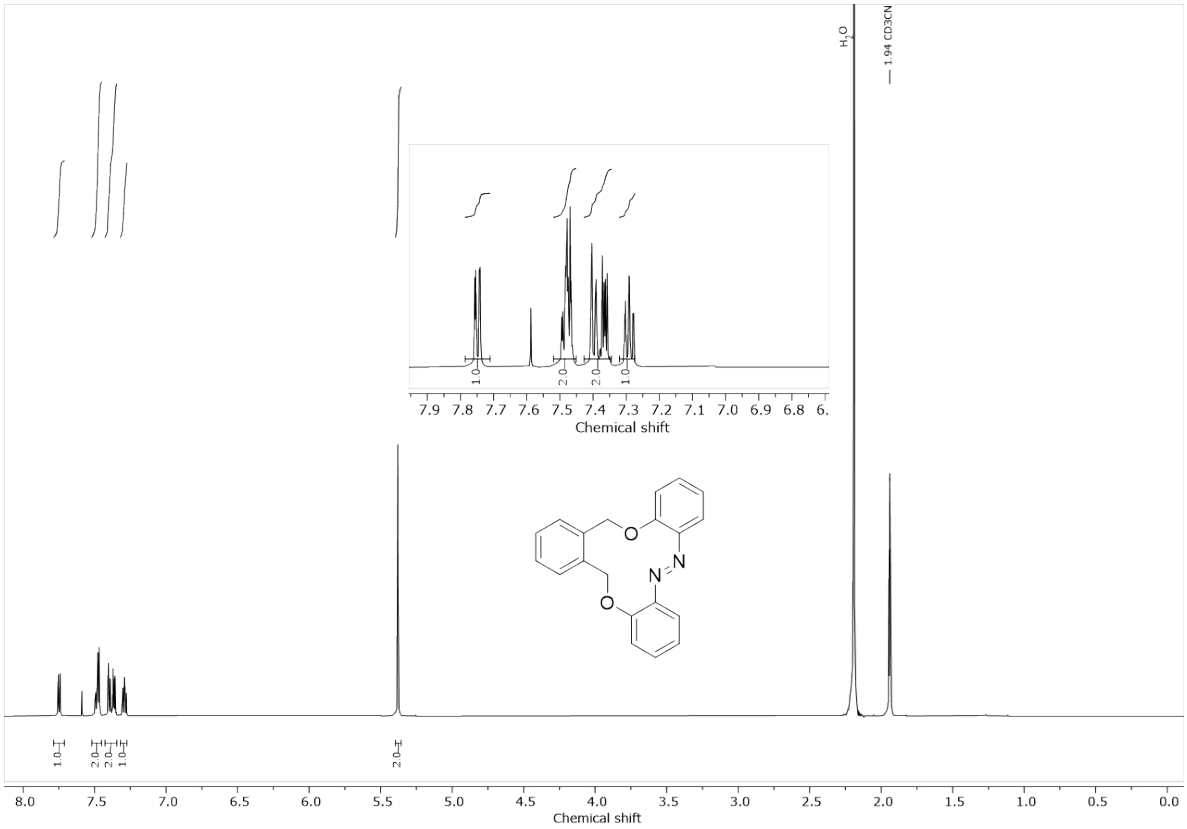


**Figure S19.** $^{1}$H NMR spectra of compound **6(*E*)** in $CD_3CN$ before irradiation.

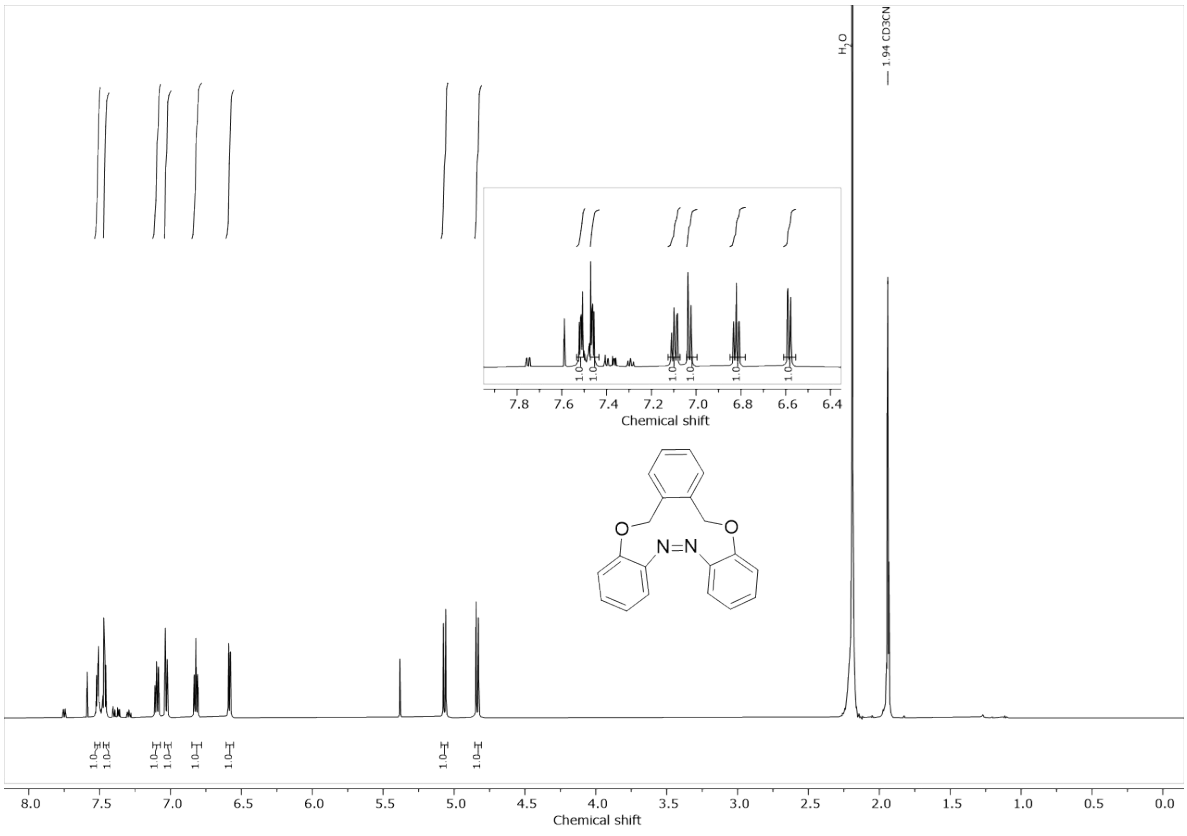


**Figure S20.** After irradiation of compound **6(*E*)** with a wavelength of 365 nm for 5 mins in the solid state and immediate dissolution in $CD_3CN$: $^{1}$H NMR of compound **6(*Z*)** in $CD_3CN$.

# 11. Collection of Macrocycles Containing the Azobenzene Motif

In the literature, there are a number of macrocyclic systems containing the azobenzene motif. Here, those systems are presented that contain either only one azobenzene and / or which have an ether linkage of the azobenzene moiety to the rest of the ring and phane structures. Also, all macrocycles containing one azobenzene with the ring sizes 12-16 are presented. In many cases, the ring closure step is not straightforward (for the yields of typical systems see Figure S21).

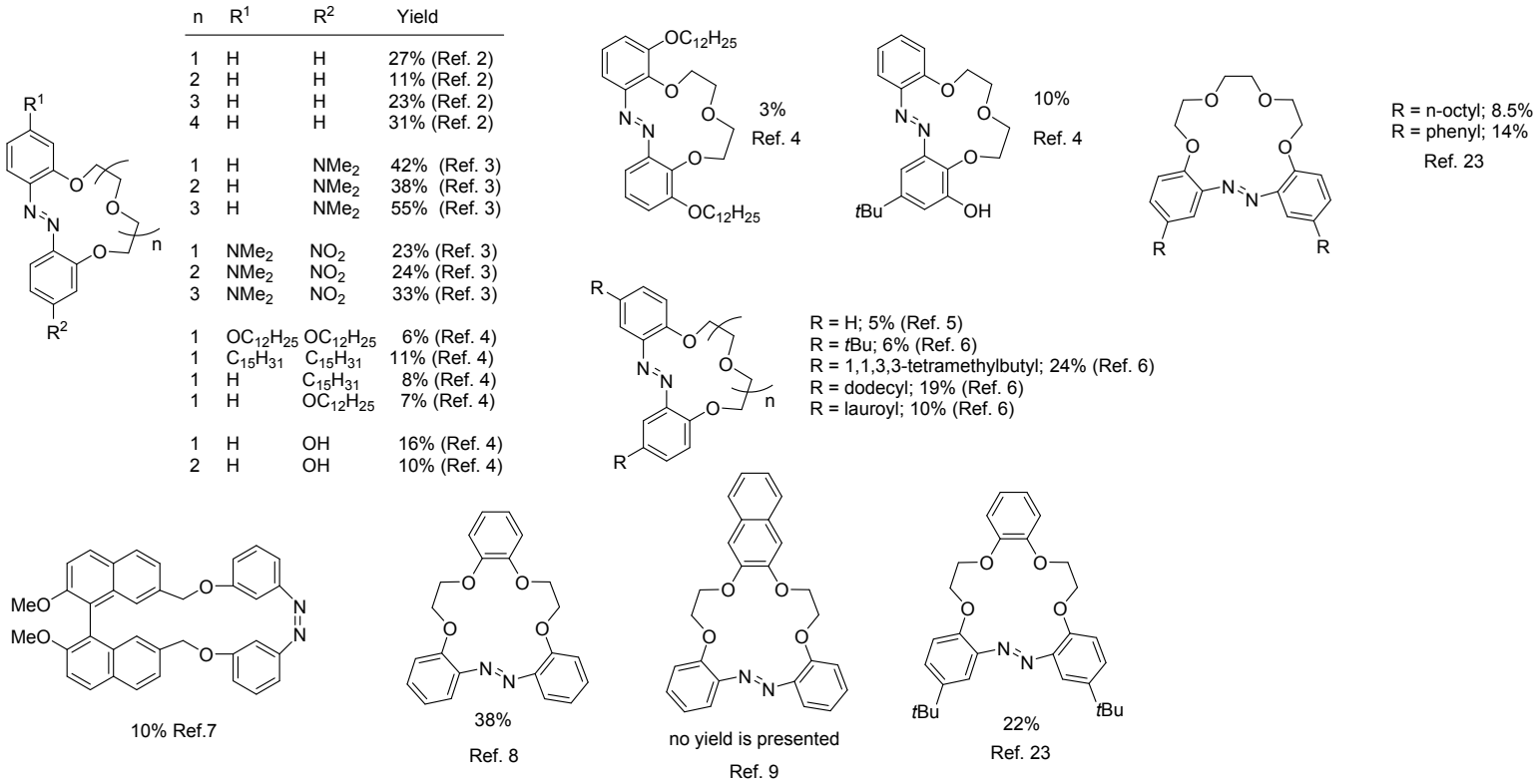


**Figure S21.** Structures with one azobenzene motif in the macrocycle, for which no photoisomerization was reported in the cited references. The yield refers to the ring closing step.

For the types of systems shown in Figure S21, the switching behaviour has often not been investigated as other properties (often complexations with ions) were the focus of the attention. Therefore, we have summed up those rings for which this analysis has been performed (Table S4).

**Table S4.** Summary of macrocyclic systems containing one azobenzene motif and their photo switching behavior.

| Compound | Isolated yield (%) | Photo-Isomerization | Absorption maxima (nm) | % PSS | Thermal relaxation | Literature citation |
|---|---|---|---|---|---|---|
| 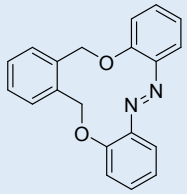 | 89 | Yes | *E*: 316; 450<br>*Z*: 290; 415 | % *E*: 88 (405 nm)<br>% *Z*: 81 (365 nm) | 20 °C,<br>> 120 days (no relaxation)<br>70 °C / $t_{1/2}$ = 36.4 h<br>90 °C / $t_{1/2}$ = 2.35 h<br>(acetonitrile) | This work |
| 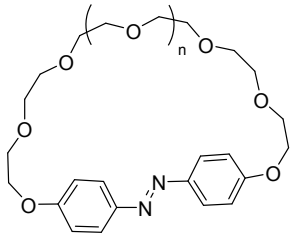 | n=1; 10.5 | Yes | 363 | %*Z*: 71.5 | 30 °C / $t_{1/2}$ = 3.0 $E^{-11}$ d<br>(*o*-dichlorobenzene) | [10] |
| | n=2; 6.3 | Yes | 363 | %*Z*: 72.5 | 30 °C / $t_{1/2}$ = 2.6 $E^{-11}$ d<br>(*o*-dichlorobenzene) | |
| | n=3; 5.0 | Yes | 361 | %*Z*: 73.6 | 30 °C / $t_{1/2}$ = 2.6 $E^{-1}$ d<br>(*o*-dichlorobenzene) | |

| | | | | | | |
|---|---|---|---|---|---|---|
| 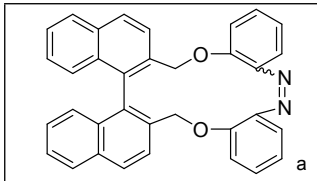 | 25 | Yes | NR | %*Z*: 86 (365 nm)<br>%*E*: 80 (436 nm) | 35 °C / $t_{1/2}$ = 1.6 d<br>(dioxane) | [7] |
| 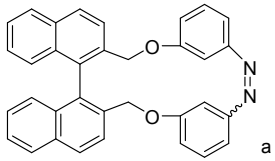 | 20 | Yes | NR | %*Z*: 78 (365 nm)<br>%*E*: 58 (436 nm) | 35 °C / $t_{1/2}$ = 0.62 d<br>(dioxane)<br>(*Z* more stable than *E*) | [7] |
| 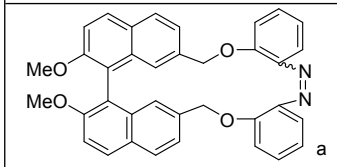 | 41 | Yes | NR | NR | 35 °C / $t_{1/2}$ = 5.35 d<br>(dioxane) | [7] |
| 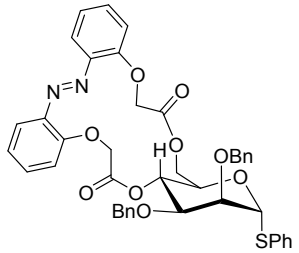 | 38 | Yes | *E*: 310;460<br>*Z*: 420 | % *E*: 53 (435 nm)<br>% *Z*: 95 (365 nm) | 25 °C / $t_{1/2}$ = 51 d<br>(acetonitrile) | [11] |
| 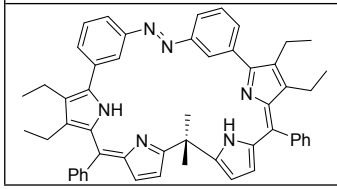 | 12 | Yes | *E*: 305, 461<br>*Z*: 298, 461 | NR | 25 ℃/ $t_{1/2}$ = 8 d<br>(toluene) | [12] |

| | | | | | | |
|---|---|---|---|---|---|---|
| 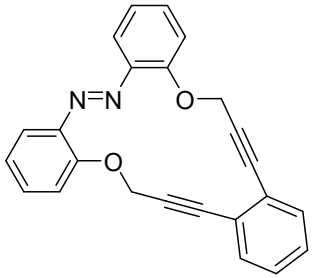 | NR | Yes | *E*: 305, 350, 440<br>*Z*: 295, 353, 438 | % *Z*: 80 | $t_{1/2}$ = 9.5 min<br>(measured in solid state by DSC)<br>(ΔT=30 ℃) | [13] |
| 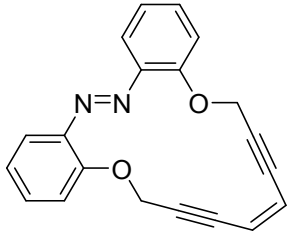 | NR | Yes | *E*: 305, 350, 440<br>*Z*: 295, 353, 438 | % *Z*: 60 | $t_{1/2}$ = 13.1 min<br>(measured in solid state by DSC)<br>(ΔT=23.4 ℃) | [13] |

a) Stereochemistry not shown.

NR: Not (explicitly) reported.

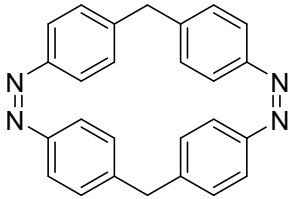

6%

Has been shown not to isomerize

Reference 14

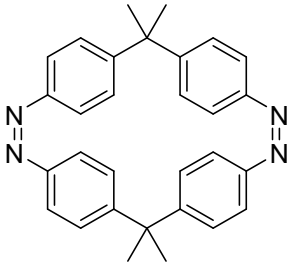

19%

Has been shown not to isomerize

Reference 15

**Figure S22.** Structures with two or more azobenzene motifs in the macrocycle for which no photoisomerization was reported in the cited references. The yield refers to the ring closing step.

**Table S5.** Selection of macrocyclic systems containing two azobenzene motifs and their photo switching behavior. As the PSS are complicated with various combinations of *E* and *Z* possible, they are not reported in this table. The yields refer to the ring closing step, which in some cases was followed by the oxidation to the actual azobenzene. In these cases, the yield for this second step to the actual product is presented in brackets.

| **Compound** | **Isolated yield (%)** | **Photo-Isomerization** | **Thermal relaxation (half life,[a] T, isomers involved)** | **Literature citation** |
|---|---|---|---|---|
| 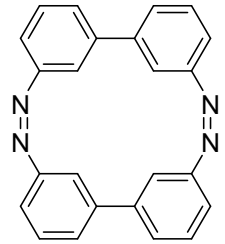 | 54%[14] (60%) | Yes[15] | full conversion after 20 days at 25 °C (*EE*→ *ZZ*) [15] | [16,17] |

| | | | | |
|---|---|---|---|---|
| 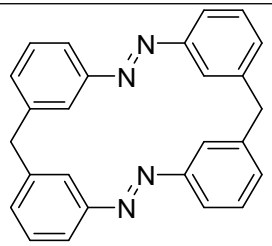 | 0.13%[16] | Yes[17] | 13.6 d at 25 °C (*Z*,*Z*→*E*,*Z*)<br>4.22 d (E,Z→EE) at 25 °C<br>(Acetonitrile)[17] | [18, 19] |
| 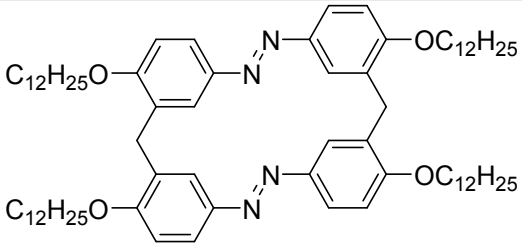 | 0.7[18] | Yes[19] | 0.3 d at 20 °C (*Z*,*Z*→*E*,*Z*)<br>0.0009 d (*E,Z*→*E,E*) at 20 °C<br>($CDCl_3$)[19] | [20,21] |
| 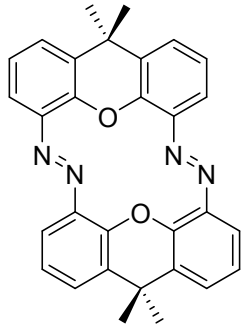 | 17 | Yes | 1600 d at 30 °C<br>(*Z*,*Z*→*E*,*Z*)<br>9.4 $E^{-4}$ d (*E,Z*→*E,E*) at 30 °C<br>(Toluene-$d_8$) | [22] |

For none of these systems apart from ours, cycle stability has been tested. It also appears that the thermal relaxation – if it has been reported – was by orders of magnitude larger than in our system.

Important requirements of azobenzene macrocyclic compound for application in solar thermal energy storage or data storage are

1. Compounds should show isomerization between the *E* and *Z* forms.
2. Compound should have high thermal stability.
3. Thermal relaxation of *Z* form to *E* form should be slow.
4. The cycle stability when switching from *E* to *Z* and vice versa should be high.

In 2019, Wegner's group successfully synthesized a series of macrocyclic oligoazobenzenes with two, three and four azobenzene units. In these, the thermal relaxation from *Z* to *E* form was relatively fast and isomerization or relaxation went through different intermediates (for example *E,Z,Z*; *E,E,Z*; *E,Z,Z,Z*; *E,E,Z,Z* etc) which made the process complicated. The authors concluded that these compounds might be important for the application in multi-stage light responsive materials and thermal relaxation can be achieved to reach up to years by increasing the number of azobenzene units (which also increase the complexicity of intermediates stage).[13]

# 12. References


1. Youn, S. W.; Lee, E. M., Metal-Free One-Pot Synthesis of N,N′-Diarylamidines and N-Arylbenzimidazoles from Arenediazonium Salts, Nitriles, and Free Anilines. *Organic Letters* **2016,** *18*, (21), 5728-5731.

2. Shiga, M.; Nakamura, H.; Takagi, M.; Ueno, K., Synthesis of Azobenzo-crown Ethers and Their Complexation Behavior with Metal Ions. *Bulletin of the Chemical Society of Japan* **1984,** *57*, (2), 412-415.

3. Luboch, E.; Wagner-Wysiecka, E.; Poleska-Muchlado, Z.; Kravtsov, V., Synthesis and properties of azobenzocrown ethers with π-electron donor, or π-electron donor and π-electron acceptor group(s) on benzene ring(s). *Tetrahedron* **2005,** *61*, (45), 10738-10747.

4. Luboch, E.; Wagner-Wysiecka, E.; Biernat, J. F., Chromogenic azocrown ethers with peripheral alkyl, alkoxy, hydroxy or dimethylamino group. *Journal of Supramolecular Chemistry* **2002,** *2*, (1), 279-291.

5. Biernat, J. F; Luboch, E.; Cygan, A.; Simonov Y. A.; Dvorkin, A. A.; Muszalska, E.; Bilewicz; R., Synthesis, x-ray structure and electrochemical properties of a new crown ether with a *cis* azo unit in the macrocycle. *Tetrahedron* **1992**, *48*, (21), 4399-4406.

6. Luboch, E.; Biernat, J. F.; Muszalska, E.; Bilewicz, R., 13-Membered crown ethers with azo or azoxy unit in the macrocycle - synthesis, membrane electrodes, voltammetry and Langmuir monolayers. *Supramolecular Chemistry* **1995**, *5*, (3), 201-210.

7. Takaishi, K.; Kawamoto, M.; Muranaka, A.; Uchiyama, M., Fusion of Photochromic Reaction and Synthetic Reaction: Photoassisted Cyclization to Highly Strained Chiral Azobenzenophanes. *Organic Letters* **2012,** *14*, (13), 3252-3255.

8. Zawisza, I.; Bilewicz, R.; Luboch, E.; Biernat, J. F., Voltammetric Recognition of *Cis* (*Z*) and *Trans* (*E*) Isomers of Azobenzene and Azocrown Ethers. *Supramolecular Chemistry* **1998,** *9*, (4), 277-287.

9. Shimizu, F. M.; Giacometti, J. A.; Luboch, E.; Biernat, J. F.; Ferreira, M., Preparation and characterization of Langmuir–Blodgett films of 16-membered azobenzocrown ether with naphthalene residue. *Synthetic Metals* **2009,** *159*, (21), 2378-2380.

10. Shinkai, S.; Minami, T.; Kusano, Y.; Manabe, O., Photoresponsive Crown Ethers. 8. Azobenzenophane-Type "Switched-On" Crown Ethers Which Exhibit an All-or-Nothing Change in Ion-Binding Ability. *Journal of the American Chemical Society* **1983,** *105*, (7), 1851-1856.

11. Lin, C.; Maisonneuve, S.; Métivier, R.; Xie, J., Photoswitchable Carbohydrate-Based Macrocyclic Azobenzene: Synthesis, Chiroptical Switching, and Multistimuli-Responsive Self-Assembly. *Chemistry European Journal.* **2017**, *23*, (60), 14996.

12. Yamamoto, T.; Nakamura, D.; Liu G.; Nishinaka, K.; Tsuda, A., Synthesis and photoisomerization of an azobenzene-containing tetrapyrrolic macrocycle. *Journal of Photochemistry and Photobiology A: Chemistry* **2016**, *331*, (8), 66-75.

13. Kar, M.; Basak, A.; Bhattacharjee, M., Photoisomerization as a trigger for Bergman cyclization: Synthesis and reactivity of azoenediynes. *Bioorganic & Medicinal Chemistry Letters* **2005**, *15*, (24), 5392-5396.

14. Heindl, A.; Schweighauser, L.; Logemann, C.; Wegner, H., Azobenzene Macrocycles: Synthesis of a *Z*-Stable Azobenzenophane. *Synthesis* **2017,** *49*, (12), 2632-2639.

15. Heindl, A. H.; Becker, J.; Wegner, H. A., Selective switching of multiple azobenzenes. *Chemical Science* **2019,** *10*, (31), 7418-7425.

16. Kang, H. M.; Kim, H. Y.; Jung, J. W.; Cho C. G., Practical Synthesis of Azobenzenophanes. *Journal of Organic Chemistry* **2007**, *72*, (2), 679–682.

17. Norikane, Y.; Katoh, R.; Tamaoki, N., Unconventional thermodynamically stable cis isomer and *trans* to *cis* thermal isomerization in reversibly photoresponsive [0.0](3,3′)-azobenzenophane. *Chemical Communications* **2008**, *16*, 1898-1900.

18. Norikane, Y.; Kitamoto, K.; Tamaoki, N., Novel Crystal Structure, *Cis−Trans* Isomerization, and Host Property of Meta-Substituted Macrocyclic Azobenzenes with the Shortest Linkers. *Journal of Organic Chemistry* **2003,** *68*, (22), 8291-8304.

19. Norikane, Y.; Tamaoki, N., Photochemical and Thermal *cis* /*trans* Isomerization of Cyclic and Noncyclic Azobenzene Dimers: Effect of a Cyclic Structure on Isomerization. *European Journal of Organic Chemistry* **2006**, *2006***,** (5), 1296-1302.

20. Norikane, Y.; Hirai, Y.; Yoshida, M., Photoinduced isothermal phase transitions of liquid-crystalline macrocyclic azobenzenes. *Chemical Communications* **2011**, *47*, (6), 1770-1772.

21. Uchida, E.; Sakaki, K.; Nakamura, Y.; Azumi, R.; Hirai, Y.; Akiyama, H.; Yoshida, M.; Norikane, Y., Control of the Orientation and Photoinduced Phase Transitions of Macrocyclic Azobenzene. *Chemistry European Journal* **2013**, *19*, (51), 17391-17397.

22. Nagamani, S. A.; Norikane, Y.; Tamaoki, N., Photoinduced Hinge-Like Molecular Motion: Studies on Xanthene-Based Cyclic Azobenzene Dimers. *Journal of Organic Chemistry* **2005**, *70*, (23), 9304-9313.

23. Luboch, E.; Biernat, J. F.; Simonov, Y. A., Dvorkin, A. A., Synthesis and electrode properties of 16-membered azo- and azoxycrown ethers. Structure of tribenzo-16-azocrown-6. *Tetrahedron* **1998**, *54*, (19), 4977-4990.